OAK RIDGE NATIONAL LABORATORY LIBRARIES
3 4456 0594449 5

ORNL/NUREG/TM-124

cy 67

Source Term Assessment Concepts for LMFBRS: Aerosol Release and Transport (ART) Analytical Program

T. S. Kress
H. W. Bertini
L. F. Parsly, Jr.
M. L. Tobias
J. S. White
A. L. Wright

Prepared for the U.S. Nuclear Regulatory Commission
Office of Nuclear Regulatory Research
Under Interagency Agreements 40-551-75 and 40-552-75

OAK RIDGE NATIONAL LABORATORY
CENTRAL RESEARCH LIBRARY
DOCUMENT COLLECTION
LIBRARY LOAN COPY
DO NOT TRANSFER TO ANOTHER PERSON
If you wish someone else to see this document, send in name with document and the library will arrange a loan.

OAK RIDGE NATIONAL LABORATORY
OPERATED BY UNION CARBIDE CORPORATION · FOR THE DEPARTMENT OF ENERGY

Printed in the United States of America. Available from
National Technical Information Service
U.S. Department of Commerce
5285 Port Royal Road, Springfield, Virginia 22161
Price: Printed Copy $6.00; Microfiche $3.00

This report was prepared as an account of work sponsored by an agency of the United States Government. Neither the United States Government nor any agency thereof, nor any of their employees, contractors, subcontractors, or their employees, makes any warranty, express or implied, nor assumes any legal liability or responsibility for any third party's use or the results of such use of any information, apparatus, product or process disclosed in this report, nor represents that its use by such third party would not infringe privately owned rights.

2/21/78

OAK RIDGE NATIONAL LABORATORY

OPERATED BY

UNION CARBIDE CORPORATION

NUCLEAR DIVISION

POST OFFICE BOX X

OAK RIDGE, TENNESSEE 37830

January 26, 1978

To: Recipients of Subject Report

Report No: ORNL/NUREG/TM-124 Classification: Unclassified

Author(s): T. S. Kress, H. W. Bertini, L. F. Parsly, Jr., M. L. Tobias, J. S. White and A. L. Wright

Subject: Source Term Assessment Concepts for LMFBRS: Aerosol Release and Transport (ART) Analytical Program.

Please correct your copy(ies) of subject report by affixing the attached correction to the front cover. It has been prepared on self-adhesive stock for your convenience, just peel off backing and affix.

J. L. Langford

J. L. Langford, Supervisor
Laboratory Records Department
Information Division

JLL:we

Attachment

ORNL/NUREG/TM-124
Dist. Category NRC-7

Contract No. W-7405-eng-26

Engineering Technology Division

SOURCE TERM ASSESSMENT CONCEPTS FOR LMFBRS: AEROSOL RELEASE AND TRANSPORT (ART) ANALYTICAL PROGRAM

T. S. Kress, Program Coordinator

Report Prepared by

H. W. Bertini
T. S. Kress
L. F. Parsly, Jr.
M. L. Tobias
J. S. White
A. L. Wright

Date Published - November 1977

Prepared for the
U.S. Nuclear Regulatory Commission
Office of Nuclear Regulatory Research
Under Interagency Agreements 40-551-75 and 40-552-75

NOTICE This document contains information of a preliminary nature. It is subject to revision or correction and therefore does not represent a final report.

Prepared by the
OAK RIDGE NATIONAL LABORATORY
Oak Ridge, Tennessee 37830
operated by
UNION CARBIDE CORPORATION
for the
DEPARTMENT OF ENERGY

OAK RIDGE NATIONAL LABORATORY LIBRARIES
3 4456 0594449 5

CONTENTS

Page

ABSTRACT v

SUMMARY vii

TITLES OF FIGURES ix

GLOSSARY OF ACRONYMS USED IN THIS REPORT xi

1. INTRODUCTION 1

1.1 References 5

2. THE HYPOTHETICAL CORE DISRUPTIVE ACCIDENT: THE END-OF-DISASSEMBLY STATE 6

2.3 References 11

3. THE MOVEMENT OF CORE DEBRIS FROM THE ORIGINAL CORE SITE TO THE LIMITS OF THE SECONDARY CONTAINMENT 12

3.1 Fragmentation of Molten Fuel During Hypothetical Core Disruptive Accidents 12

3.1.1 Introduction 12

3.1.2 Occurrence of Fragmentation and its Impact on Source Term Calculations 12

3.1.3 Previous Work 14

3.1.3.1 Hydrodynamic fragmentation 14

3.1.3.2 Thermal fragmentation 19

3.1.4 Work Plan 19

3.1.5 References 22

3.2 Effects of the Passage of the Disassembled Core-Fuel Mixture through the Upper Core Structure 23

3.2.1 Introduction 23

3.2.2 Description of Expansion through the Structure 23

3.2.3 Previous Work 27

3.2.4 Work Plan 28

3.2.5 References 29

3.3 Expansion of the Core Bubble Into the Sodium Pool . . . 31

3.3.1 Time Independent Expansion Thermodynamics 31

3.3.1.1 Introduction 31

3.3.1.2 Related work 32

3.3.1.3 Work plan 33

3.3.1.4 Results to be obtained 34

3.3.1.5 References 35

Page

3.3.2 Time Dependent Expansion Following Disassembly 36
3.3.2.1 Introduction 36
3.3.2.2 Related work 36
3.3.2.3 Work plan 37
3.3.2.4 References 38

3.4 Thermal Effects as the Bubble Rises Through the Sodium Pool 40

3.4.1 Introduction 40
3.4.2 Proposed Simplified Thermal Model 41
3.4.2.1 Temperature potentials 43
3.4.2.2 Heat transfer coefficients 45
3.4.2.3 Effects of radiant heat 48

3.4.3 Source Considerations Related to Thermal Modeling 49
3.4.4 References 50

3.5 Aerosol Formation and Attenuation in the Rising Bubble and the Cover Gas Region 51

3.5.1 References 53

3.6 Aerosol Formation and Attenuation in Leakage from the Primary Containment 54

3.6.1 General Remarks 54
3.6.2 Attenuation of Aerosols due to Plugging 54
3.6.3 Aerosol Generation During Free Expansion 55
3.6.4 Work Plan 56
3.6.5 References 57

3.7 Aerosol Behavior in the Secondary Containment 59

3.7.1 General Remarks 59
3.7.2 Computer Codes for Secondary Containment Analysis 60
3.7.3 References 63

ABSTRACT

Analytical needs for LMFBR HCDA source term assessment are outlined and the physical events connected with the formation of an aerosol source are discussed. The important features of the movement of hazardous materials from the core site to the boundaries of the secondary containment are described, with accompanying brief reviews of prior work. The overall problem is broken down into tractable parts and approaches for attacks on the various problems are suggested. Topics include the state of the disrupted core, interactions with intact above-core structure, HCDA bubble formation, heat exchange with the sodium pool, aerosol formation by nucleation and fragmentation, attenuation effects, and aerosol behavior in secondary containments.

SUMMARY

This outline of source term assessment needs follows the possible course of a core material-coolant mixture from the site of a hypothetical disruption to the boundaries of the secondary containment. The high-temperature, high-pressure, multi-phase mixture of sodium and core material produced by the HCDA is assumed to pass through the remains of the upper core structure, through the sodium pool and into the cover gas region. This material is assumed to subsequently leak into the air-filled secondary containment where it may undergo further changes. This is the material which can potentially leak into the environment. The composition and state of this mixture are determined by the physical and chemical events which take place along the way, as well as by the history of the reactor up to the time of the accident. An attempt is made to point out the important contributory phenomena and suggest ways in which they can be studied; the ultimate aim is the preparation of practical engineering calculational methods to characterize the properties of the aerosol mixture in the secondary containment.

Sections of this report discussing the above topics were prepared by individual staff members more or less independently of one another but with overall guidance provided by the program coordinator. A list of issues which are important to examine follows. (The parenthetical numbers refer to the sections where the topic is discussed.)

1. What is the state of the core at the end of disassembly? (2)
2. What effect will fragmentation processes have on the potential source? (3.1)
3. What changes occur to the disassembled core mixture of materials as it moves through the above-core structure? (3.2)
4. What is the bubble's initial thermodynamic state? (3.3)
5. What effects are produced by heat exchange between the bubble and the sodium? (3.4)
6. How does the aerosol suspension behave in the bubble and in the cover gas region? (3.5)

7. What are the effects on aerosol characteristics due to blockage? (3.6)
   a. What alteration may be expected from plugging? (3.6.2)
   b. What changes take place in the aerosol on free expansion into the secondary containment? (3.6.3)
8. What is the behavior of aerosols in the secondary containment? (3.7)

Those aspects of the proposed analytical activity that are connected to the ART experiment programs in the CRI-II, CRI-III/CDV, NSPP, and FAST facilities are indicated.

TITLES OF FIGURES

		Page
Fig. 1.	Schematic LMFBR Diagram, taken from the TLTM report for the CRBR, illustrating various aspects of the ART Program	2
Fig. 2.	Comprehensive mechanistic accident analysis path structure	7
Fig. 3.	Situations in which fragmentation may occur	13
Fig. 4.	The fragmentation mechanism	15
Fig. 5.	Fragmentation classification	17
Fig. 6.	Thermal fragmentation	20
Fig. 7.	Initial state of the disassembled core	24
Fig. 8.	(a) Sodium expansion, fuel breakup and entrainment; (b) fuel expansion, fuel breakup and entrainment	26
Fig. 9.	Temperature and concentration fields at the interface of an HCDA Bubble	46

GLOSSARY OF ACRONYMS USED IN THIS REPORT

ART	Aerosol Release and Transport
BEC	Beginning of Equilibrium Cycle
CRBR	Clinch River Breeder Reactor
EEC	End of Equilibrium Cycle
FAST	Fuel Aerosol Simulant Test
FCI	Ruel-Coolant Interaction (thermal)
FFTF	Fast Flux Test Facility
HCDA	Hypothetical Core Disruptive Accident
LMFBR	Liquid Metal Fast Breeder Reactor
TLTM	Third Level Thermal Margins
TOP	Transient Overpower
TUC	Transient Undercooling

SOURCE TERM ASSESSMENT CONCEPTS FOR LMFBRS: AEROSOL RELEASE AND TRANSPORT (ART) ANALYTICAL PROGRAM

T. S. Kress, Program Co-ordinator

1. INTRODUCTION

M. L. Tobias

The preparation of this document has been guided in terms of response to a basic practical problem which can be stated as follows:

> Safety analysis reports prepared as part of the licensing process for LMFBRs must evaluate the radiological consequences of hypothetical core disruptive accidents. What information must the regulatory staff have in order to assess the validity and merits of these evaluations?

In response to this need, a program of analytical studies has been outlined to assess the radiological source resulting from an HCDA.

To fix ideas, we refer now to Fig. 1, a schematic based on recent CRBR concepts. A person at point M is presumed to be exposed to a radioactive dose originating from a core disruptive accident. The amount of exposure will be a function of both position and time. The source of this exposure arises out of core materials which have been released into the reactor containment building and which escape through the secondary containment structures 3 and 4. The radioactive source material enters the reactor containment building due to openings or leaks in the reactor enclosure system (defined as the reactor vessel, the closure head, and the guard vessel).* The enclosure system has become a repository of radioactive source material dispersed from the core as a result of accidents which may melt and vaporize some portion of the fuel.

Various causes might be hypothesized for the openings to exist in the primary containment, such as melt-through due to core debris deposited

---

*The "parallel design" mentioned in Ref. 1 and the PSAR for the CRBR also included a sealed head access area. This feature is not included here.

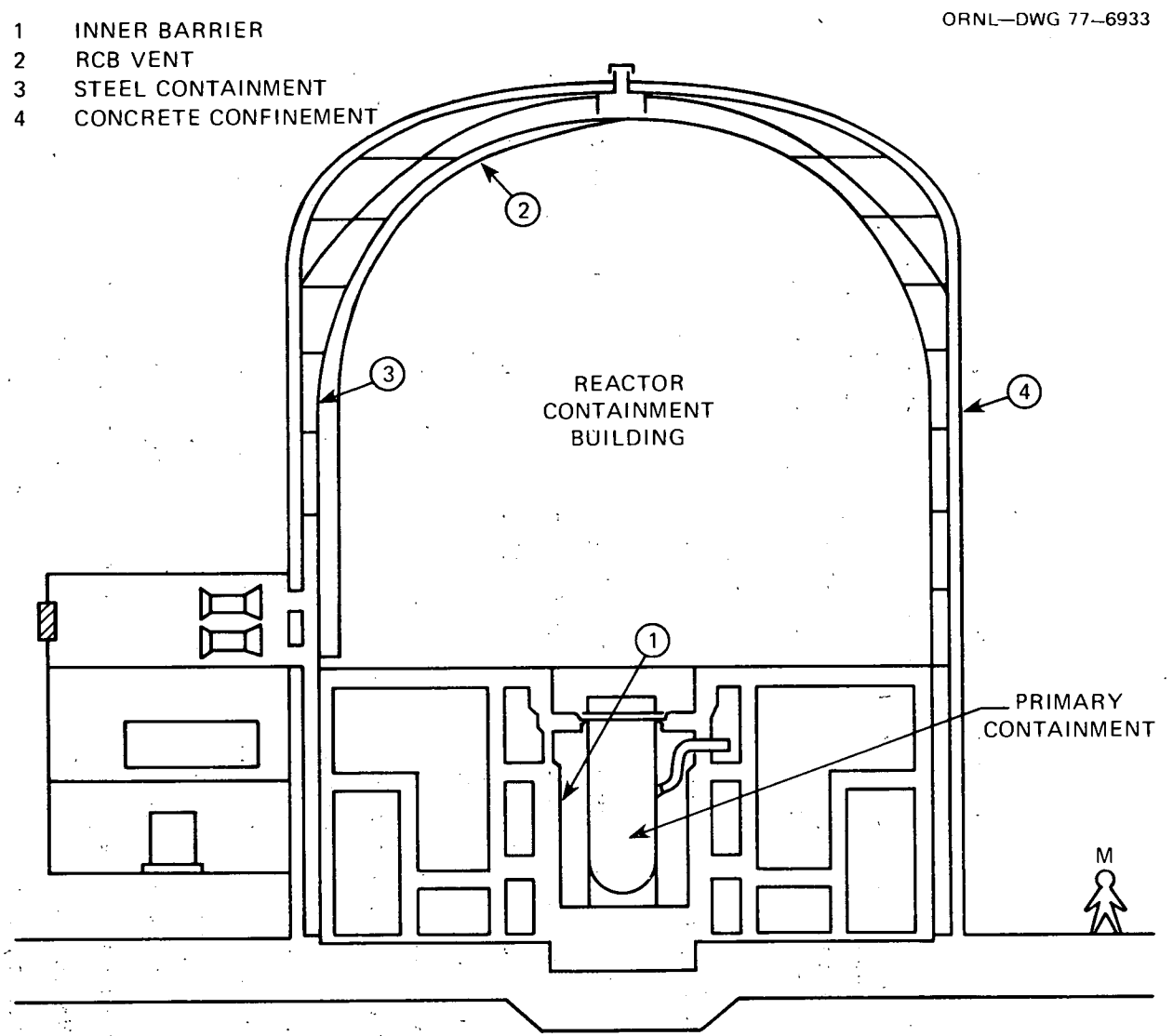

Fig. 1. Schematic LMFBR Diagram, taken from the TLTM report for the CRBR, illustrating various aspects of the ART Program.

on the vessel, a power excursion energetic enough to open the pressure vessel head,* or even earthquakes or sabotage.

At present it is not clear what events should be admitted as causes or radioactive material releases. Therefore, in the ART program it is proposed that leaks of unspecified size be considered without specifying the sequence of events leading to the creation of the leaks. Calculational procedures will then be developed to determine the release rates and the behavior of the resulting aerosols for ranges of conceivable physical conditions which might occur in an accident. (A similar approach has been taken by others.)[4] Initiating accident mechanisms will be considered for background information only. The source characterization problem will be broken into tractable parts by concentrating on the important physical phenomena following the cessation of power generation.

Starting with arbitrary but representative values for the thermodynamic states of the core following postulated power excursions, leaks will be assumed to exist in the primary containment system that will allow material to be released into the reactor containment building. The principal questions to be addressed then are the following:

1. Reactor core material is assumed to be transported from the original core position in the form of a "bubble" (or "bubbles") having several components in various forms: solid fragments, aerosols, droplets, vapor, etc. The initial composition, temperature and pressure are related to the total quantity and distribution of excess energy deposited in the molten fuel. How do the mechanisms of formation of this bubble affect its

---

*There is considerable divergence of view concerning the likelihood of such events. For example, Ref. 2 contains a statement that a hypothetical core disruptive accident should not be considered as a design basis accident. At the opposite (and anti-nuclear) extreme, Ref. 3 claims that explosive LMFBR accidents are conceivable which could require abandonment of a 150 000 sq. mile area.

initial composition and what changes will occur in the bubble as it rises through the sodium and the structure above the core into the cover gas area?

2. What is the aerosol behavior of the material in the bubble and the cover gas area before leakage to the secondary containment?

3. What changes may be expected to occur as the material in the primary containment enters the secondary containment through leakage paths of various lengths and cross sections?

4. What is the behavior of the aerosols in the secondary containment region arising from:
   a. burning sodium;
   b. release of mixed oxide fuels;
   c. release of fission products?

   In particular what are the effects of the timing, magnitude, and rates of release into the secondary containment environment upon aerosol behavior? (By behavior we mean aerosol composition and properties, rates of coagulation, settling, wall deposition, and resuspension.)

In the light of the original basic aim, this document has two primary purposes: first, to outline a proposed program of analytical studies; second, to serve as a general guide to those physical phenomena which occur during an LMFBR core disruptive accident which we believe to be of significance in the generation of an aerosol source and to list the physical problems associated with these phenomena. Introductory material is then followed by discussions of the individual phenomena by the staff members directly concerned with each area. Suggested plans of analyses are intended to reflect a basic philosophy that, for the purposes of a safety assessment, bounds, as well as best estimates, on the physical phenomenon are appropriate. In developing this analytical program we recognize that significant contributions are being made by other

participants for the Nuclear Regulatory Commission as well as in work sponsored by ERDA. Our efforts are intended to be collaborative and complementary rather than competitive.

1.1 REFERENCES

1. John Graham, Nuclear Safety 16 No. 5, p. 579, Sept-Oct 1975.

2. Letter, R. P. Denise to Lochlin W. Caffey, May 6, 1976, p. 5.

3. The Accident Hazards of Nuclear Power Plants, Richard E. Webb, The University of Massachusetts Press, Amherst 1976, p 118.

4. J. A. Gieseke et al., Analytic Studies of Aerosol Behavior Predictions for Fast Reactor Safety, BMI-1932, March 19, 1975 Battelle Columbus Laboratories.

2. THE HYPOTHETICAL CORE DISRUPTIVE ACCIDENT: THE END-OF-DISASSEMBLY STATE

J. S. White

Recent efforts to develop mechanistic approaches for analyzing core disruptive accident sequences for the CRBR and FFTF have led to the identification of three accident progression paths (Fig. 2).[2] The first is an early termination path due to negative-reactivity effects. In other paths, the accident could proceed directly to an energetic disassembly or, alternatively, enter a transition phase where shutdown may be caused by either mild fuel dispersal or an energetic disassembly.

Accident sequences depend strongly on specific reactor configurations. Thus, several differences exist between the CRBR and the FFTF which result in different accident scenarios. It is difficult to suppose realistic mechanisms for energetic disassemblies for the FFTF, whereas there are combinations of pessimistic assumptions that can be made for the CRBR to produce a calculated hydrodynamic disassembly directly from initiating phases. The mechanistic approach has been described in detail in references (1) and (2) for CRBR accident scenarios of both transient undercooling (TUC) and transient overpower (TOP) initiating events with failure of both primary and secondary safety systems. Four best estimate base cases were analyzed using the current versions of SAS3A[3,4] and VENUS-II [5] based on the TUC and TOP accidents under both beginning of equilibrium fuel cycle (BEC) and end-of-equilibrium fuel cycle (EEC) conditions. Five parametric cases were run as variations from these base cases to determine the effects of pessimistic assumptions on total energy generation.

Hydrodynamic disassembly conditions were obtained in one of these parametric SAS3A calculations for a TUC base case with a BEC core. These conditions of high core temperatures, high power level, and a large sustained ramp rate were used for a voided-core VENUS-II calculation and calculation of the fuel expansion work (Table 2.1).[2]

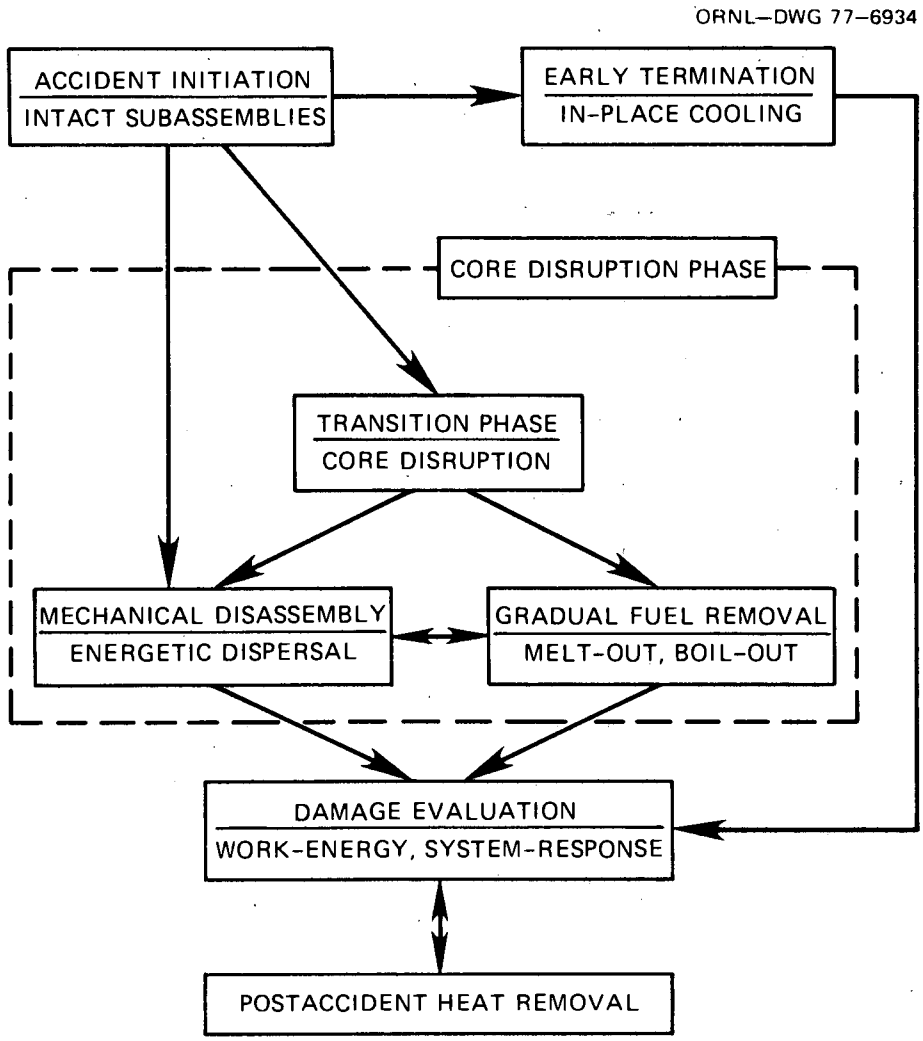

Fig. 2. Comprehensive mechanistic accident analysis path structure.

Table 2.1. Initiating accident scenario — Summary of disassembly calculation for beginning-of-equilibrium-cycle transient undercooling accident

a.	Initial Conditions	
	Core average temperature	2992 K
	Reactivity	1.07 $
	Power	4.28×10^{11} watts (440 × nominal)
	Ramp	50 $/second
b.	VENUS-II Results	
	Core average temperature	4150 K
	Maximum temperature	5797 K
	Energy in molten fuel	5560 MJ
c.	Fuel Expansion Work	
	Work-energy to 2.1×10^7 cm^3 "Na-slug impact"	72 MJ
	Work-energy to 1 atm	350 MJ

Three additional variations on this case were run with 75 and 100 dollars per second ramp rates. In addition the effect of increasing the Doppler coefficient was examined. The VENUS-II results and the fuel expansion work[2] are summarized in Table 2.2.

The conclusions drawn from these accident scenarios were that a highly energetic disassembly accident would require either postulated large ramp rates or autocatalytic fuel compaction, neither of which is currently thought probable. However, because of uncertainties in the computer calculated results, a conservative approach should be taken by using a range of values for the post-disassembly state in the neighborhood of the CRBR bounding case as initial conditions for subsequent source term analyses.

Table 2.2. Summary of parametric disassembly calculations

a VENUS-II Results	75$/second	100$/second	100$/second*
Core average temperature (K)	4483	4802	4533
Maximum temperature (K)	6300	6857	6357
Energy in molten fuel (MJ)	6690	7700	6860

b Fuel Expansion Work	75$/second	100$/second	100$/second*
Work-energy to 2.1×10^7 cm^3 "Na-slug impact" (MJ)	126	194	131
Work-energy to 1 atm (MJ)	591	974	632

*Run with increased Doppler as explained in the text.

2.3 References

1. Clinch River Breeder Reactor Plant, Preliminary Safety Analysis Report, Project Management Corporation.

2. W. R. Bohl et al., An Analysis of Transient Undercooling and Transient Overpower Accidents Without Scram in the Clinch River Breeder Reactor, ANL/RAS 75-29, Argonne National Laboratory, July 1975.

3. M. G. Stevenson et al., "Current Status and Experimental Basis of the SAS LMFBR Accident Analysis Code Systems," in Proceedings of a Conference on Fast Reactor Safety, Beverly Hills, California, April 1974, Report CONF-740401-P3, Vol. 3, pp. 1393–1321.

4. F. E. Dunn et al., The SAS3A LMFBR Accident Analysis Computer Code, ANL/RAS 75-17 (1975).

5. J. F. Jackson and R. B. Nicholson, VENUS-II: An LMFBR Disassembly Program, ANL-7951 (1972).

3. THE MOVEMENT OF CORE DEBRIS FROM THE ORIGINAL CORE SITE TO THE LIMITS OF THE SECONDARY CONTAINMENT

3.1 Fragmentation of Molten Fuel During Hypothetical Core Disruptive Accidents

A. L. Wright

3.1.1 Introduction

For HCDA releases attributable to buoyant rise of vapor bubbles, the primary concern is with fuel that has been vaporized along with volatile and gaseous fission products. However, if mechanisms exist whereby quantities of liquid fuel can be fragmented into small sizes, these could contribute to the radiologic source term as well as influence the behavior of the HCDA bubble. The goal of this section, then, is to examine postulated fragmentation mechanisms and propose methods to estimate the sizes of fuel fragments that might result.

3.1.2 Occurrence of Fragmentation and Its Impact on Source Term Calculations

There seem to be two general fragmentation mechanisms postulated for HCDAs:

1. "Hydrodynamic" fragmentation, or liquid breakup due to the relative motion of fluid across a liquid surface.
2. "Thermal" Fragmentation, or breakup of fuel due to stresses produced by solidification of liquid fuel due to contact with sodium coolant.

Some of the situations during which fragmentation may occur are shown in Fig. 3. These situations have been discussed by Reynolds, et al.,[2] Buttery,[3] and Cronenberg and Grolmes:[13]

a. Fuel may jet out of a ruptured fuel pin. Rayleigh[1] showed that at a critical velocity, liquid jets become unstable and break up; the resulting droplet radius is

$$R_{drop} \simeq 1.9 \; R_{jet} \; . \qquad (1)$$

b. Fuel drops may contact sodium coolant and freeze. The fuel may then fragment due to thermal stresses.

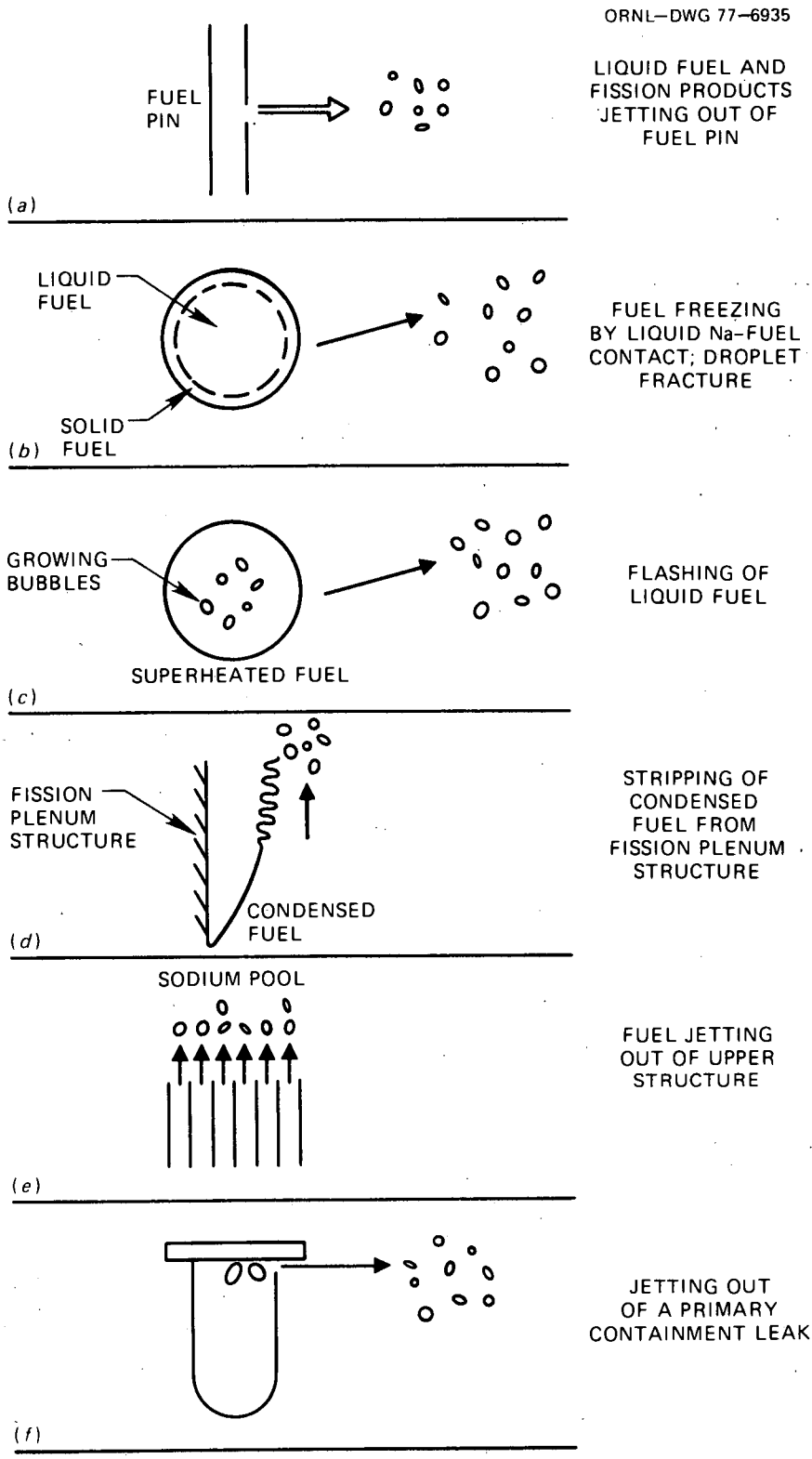

Fig. 3. Situations in which fragmentation may occur.

c. After disassembly, the high pressure, high temperature fuel mixture may rapidly evaporate, or "flash." The accelerations and shear forces resulting from rapid growth of vapor bubbles may efficiently fragment the residual liquid.

d. Fuel vapor may condense as a film on the fission gas plenum (see section 3.3). The vapor that streams past the film can strip droplets from it.

e. The jetting of two-phase fuel out of the fission plenum may result in small droplets of fuel being formed.

f. Liquid drops and aerosol particles jetting out of a leak in the primary containment into the secondary containment may break up.

Fragmentation could significantly affect the magnitude of the aerosol source term. First of all, it can influence the content of the rising HCDA vapor bubble. If many small drops become well mixed with sodium coolant in the core, the fuel may lose significant quantities of heat to the sodium because of the large heat transfer area. Such a fuel-coolant interaction may lead to larger peak pressures and result in a bubble containing large amounts of sodium vapor.

If small aerosol-like fragments are formed during the fuel mixture expansion, they may be carried up in the bubble and be a significant part of the source term. Finally, if liquid or solid materials fragment when passing through a primary containment leak, the nature and hazard of the source may be altered significantly.

3.1.3 Previous Work

3.1.3.1 Hydrodynamic fragmentation

Hydrodynamic fragmentation (Fig. 4) results when hydrodynamic forces exerted on a drop exceed the restoring surface tension force. Various hydrodynamic mechanisms leading to fragmentation were described by Buttery[3] and further described by Reynolds et al.[2] Three dimensionless parameters are important in determining how hydrodynamic fragmentation occurs:

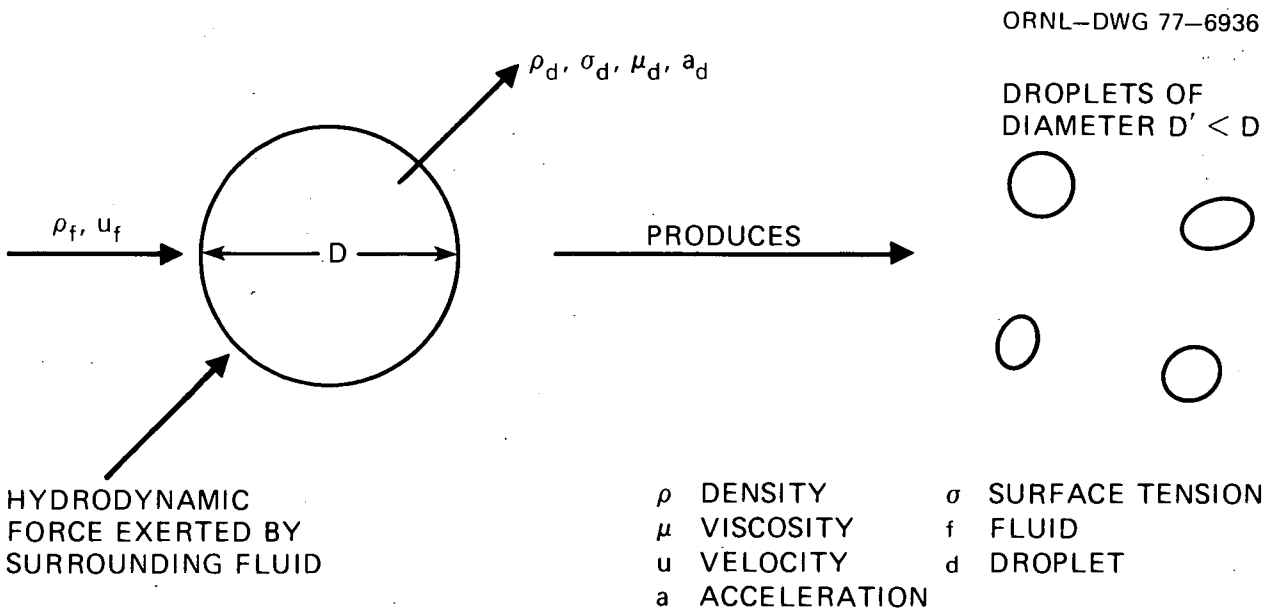

Fig. 4. The fragmentation mechanism.

Weber Number: We = inertial forces/surface tension forces

$$We = \rho_f (u_f - u_d)^2 D/\sigma_d \tag{2}$$

Viscosity Number: $Vi = \dfrac{\text{viscous forces}}{\text{surface tension forces}} \times \dfrac{\text{viscous forces}}{\text{inertial forces}}$

$$Vi = \mu d/\sqrt{\rho_d \sigma_d D} \tag{3}$$

Bond Number: Bo = acceleration forces/surface tension forces

$$Bo = \rho_d a_d D^2/\sigma_d \tag{4}$$

and $Bo = \frac{3}{4} C_D We$

C_D = drag coefficient for flow around a sphere of diameter D.

Four types of hydrodynamic fragmentation are illustrated in Fig. 5, adapted from Buttery.[3] Above a critical Weber number, drops distort and break due to aerodynamic forces.[4] Liquid viscosity has a stabilizing effect on this breakup: the viscosity number accounts for this. Aerodynamic breakup is characterized by "algebraic" (i.e., continuous and stable) drop deformation, as contrasted with instability breakup.

For greater Weber and Bond numbers, up to Bo $\sim$10, boundary layer stripping and capillary wave breakup may occur. Boundary layer stripping[5,6] results when liquid layers are stripped from the surfaces of drops. An estimate of the boundary layer thickness, δ_1, and so the size of stripped droplets can be obtained from the work of Ranger and Nicholls:[5]

$$\delta_1 = \left\{ \frac{2\pi D(\mu_d/\rho_d)}{3u_f(\mu_f\rho_f/\mu_d\rho_d)^{1/3}} \right\}^{1/2} \tag{5}$$

ORNL–DWG 77–6937

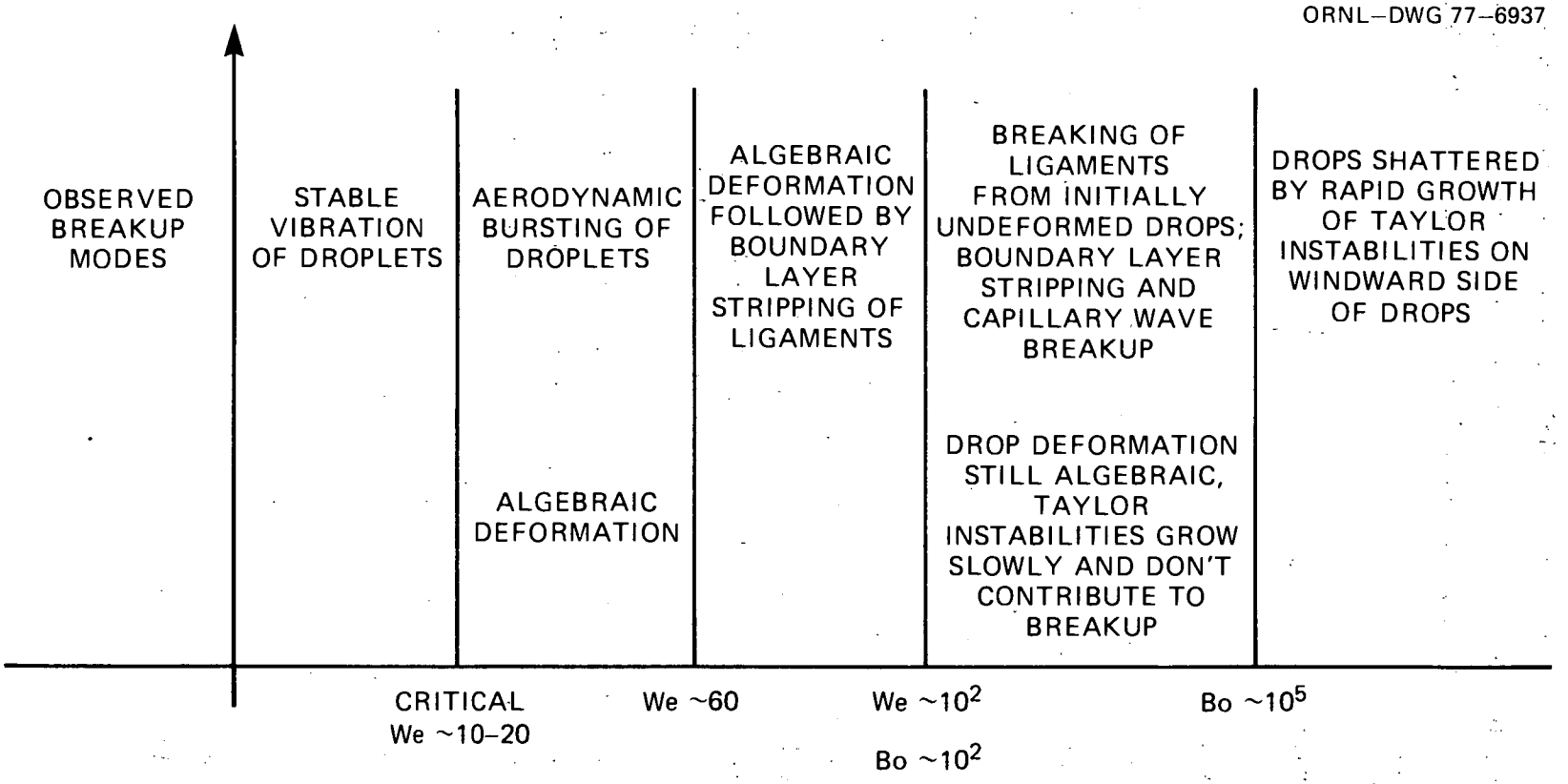

Fig. 5. Fragmentation classification.

Capillary waves[7,8] are Kelvin-Helmholtz waves generated on a liquid surface due to a flowing gas. Mayer[7] found that a minimum wavelength could be excited to high amplitudes and break from the liquid; this minimum wavelength is

$$\lambda_m = 2\pi(16)^{1/3}\left[\mu_d(\sigma/\rho_d)^{1/2}\ \beta\rho_f u_f^2\right]^{2/3} \tag{6}$$

$$\beta \sim .3$$

The mean fragment diameter is proportional to λ_m.

For Bond numbers less than 10^5, Taylor instabilities[9] grow, but their growth is slow and they do not influence breakup. When Bo > 10^5, however, these instabilities grow rapidly and shatter liquid drops abruptly.[6,10]

Additionally, liquid fuel may be fragmented by flashing, due to rapid growth of vapor bubbles within the liquid. Brown and York[12] investigated the break-up of flashing liquid jets and found that above a critical superheat the jet shattered due to vapor bubble growth. The mechanism of breakup is not clear, i.e., aerodynamic bursting, Taylor instability, etc.

Conceivably, liquid fragment sizes could be calculated on the basis of Bond and Weber numbers for a flow. Another means would be to use an empirical correlation for drop sizes, valid for a wide range of conditions, such as that developed by Isshiki[11]

$$(D'/D)^{0.25} = 1.9/(We)^{0.25} + 0.315(\rho_f/\rho_d)^{0.5}$$

$$C_D(We)^{0.125}\ln(D/D') \tag{7}$$

D = initial drop size

D′ = final drop size

3.1.3.2 Thermal fragmentation

A thermal fragmentation process, following Cronenberg and Grolmes description,[13] is illustrated in Fig. 6. When liquid sodium and liquid fuel drops contact, fuel may freeze at its outer surface. Large thermal stresses may result which exceed the fuel yield stress and fragment the drop.

Calculations discussed by Cronenberg and Grolmes indicate that the "homogeneous crystallization" temperature, below which UO_2 should solidify, is 2373 K, about 700 K below the UO_2 melting point. If the interface temperature that results on contact of liquid fuel and sodium is below this value, interface solidification of the outer shell of the UO_2 droplet should result. The thermal stresses produced due to severe thermal gradients can be calculated using a known solution for the thermoelastic stress produced in a molten sphere.[14] Such stresses calculated by Cronenberg and Grolmes were large enough to fracture the drop; however, no final drop sizes were predicted.

In the view of Cronenberg and Grolmes,[13] if liquid fuel – liquid sodium contact occurs, thermal fragmentation is the dominant break-up mechanism, as opposed to hydrodynamic fragmentation.

3.1.4 Work Plan

To determine the particle sizes that result from fragmentation, the following work appears to be necessary:

a. Determine physical conditions existing during various phases of HCDA's: pressures, jet velocities, bubble growth rates for flashing, possibility of fuel-sodium liquid contact, drop sizes before fragmentation, etc.

b. Using "a" as input conditions, determine the mode of fragmentation that occurs, whether thermal or hydrodynamic fragmentation. Use empirical correlations or develop schemes to calculate the particle sizes produced on the basis of Bond and Weber numbers.

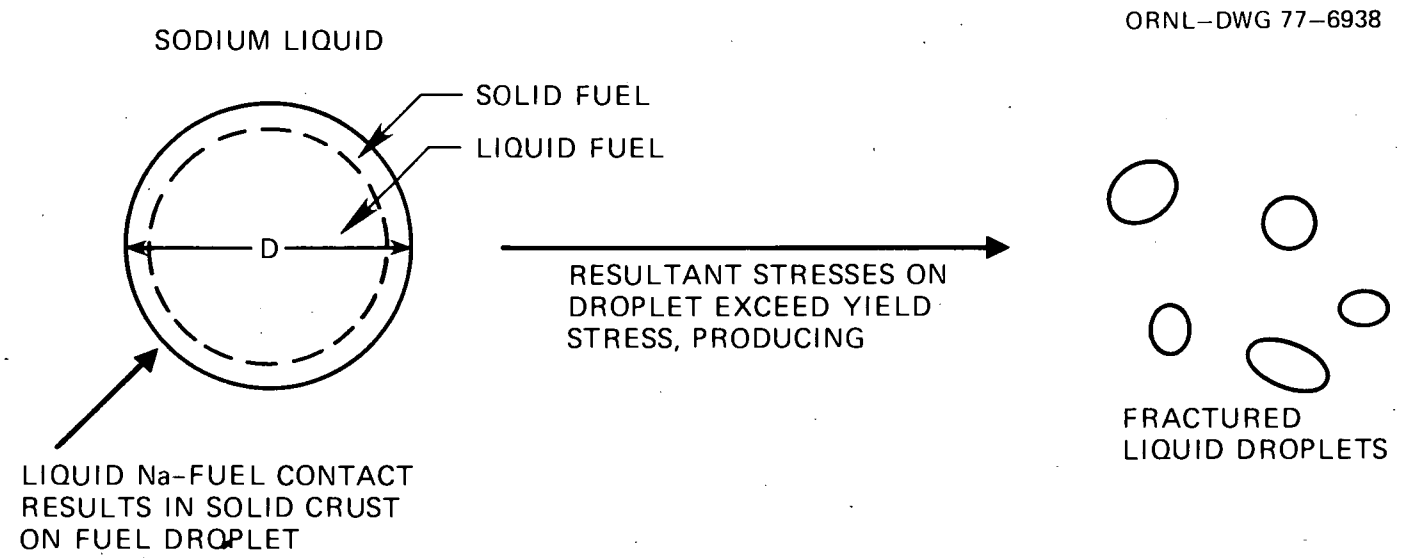

Fig. 6. Thermal fragmentation.

c. Compare caluclated drop sizes with those found in HCDA experimental programs. Scaling may not be realistic in all cases; for instance, fuel flashing at a few hundred atmospheres down to 1—20 atmospheres in the primary containment may not be analogous to the flashing of water jets at much lower pressures.[12]

The CRI-III and FAST experiments of the ART Program[15] can be important sources for HCDA particle size data. In CRI-III, UO_2 flashes in an argon atmosphere; in FAST, liquid UO_2-sodium contact may occur during flashing. If measurements of the fragment sizes produced can be made, this would be most valuable in guiding development of models, testing their validity, and in determining the dominant fragmentation process for liquid-liquid contact.

3.1.5 References

1. G. B. Wallis, One-Dimensional Two-Phase Flow, McGraw Hill, 1969, p. 376.
2. A. B. Reynolds, et al., Bubble Behavior in LMFBR Core Disruptive Accidents, University of Virginia Annual Report, June 1, 1975—June 30, 1976, NUREG-0114 (Sept. 1976).
3. N. E. Buttery, Possible Aerosol Formation Mechanisms Following LMFBR Whole Core Accidents, RD/BN 3497 (Rev), Berkeley Nuclear Laboratories (January 1976).
4. J. O. Hinze, "Fundamentals of the Hydrodynamic Mechanism of Splitting in Dispersion Processes," A.I.Ch.E. Journal, 1, 289 (1955).
5. A. A. Ranger, J. A. Nicholls, "Aerodynamic Shattering of Liquid Drops," AIAA Journal, 7, 285 (1969).
6. E. Y. Harper, G. W. Grube, I-Dee Chang, "On the Breakup of Accelerating Liquid Drops," J. Fluid Mech., 52, 565 (1972).
7. E. Mayer, "Theory of Liquid Atomization in High Velocity Gas Streams," ARS Journal, 31, 1783 (1961).
8. M. A. Weiss, C. H. Worsham, "Atomization in High Velocity Airstreams," ARS Journal, 29, 252 (1959).
9. G. I. Taylor, "The Instability of Liquid Surfaces when Accelerated in a Direction Perpendicular to their Planes. I," Proc. Roy. Soc. (London), A 201, 192 (1950).
10. P. G. Simpkins, E. L. Bales, "Water-Drop Response to Sudden Accelerations," J. Fluid Mech., 55, 629 (1972).
11. N. M. Isshiki, Rept. 35, Transportation Technical Research Institute, Tokyo, Japan (July 1959).
12. R. Brown, J. L. York, "Sprays Formed by Flashing Liquid Jets," A.I.Ch.E. Journal, 8, 149 (1962).
13. A. W. Cronenberg, M. A. Grolmes, "Fragmentation Modeling Relative to the Breakup of Molten UO_2 in Sodium," Nucl. Safety, 16, 683 (1975).
14. J. Nowinski, "Thermoelastic Problem for an Isotropic Sphere with Temperature-Dependent Properties," Z. Angew. Math. Phys., 10, 565 (1959).
15. T. S. Kress, G. W. Parker, M. H. Fontana, Work Plan: Transient Release Program, ORNL-TM-4875, Oak Ridge National Laboratory (1975).

3.2 Effects of the Passage of the Disassembled Core Fuel Mixture Through the Upper Core Structure

A. L. Wright

3.2.1 Introduction

Questions addressed in this section are related to mechanisms which may attenuate or increase the aerosol source term as the disassembled LMFBR fuel mixture expands through the upper core structure of the reactor. This mixture can be assumed originally to be made up of molten fuel and steel, sodium, and fission gases. The expansion process and composition of the vapor bubble will be influenced by the heat exchange between molten fuel and sodium coolant that may be still present in the core. In addition, the upper core has been taken to be as much as four thousand degrees (°F) cooler than the molten core[15], so possible energy losses from the expanding core to the structure may strongly attenuate the source. Additions to the source term may result if the expanding mixture entrains fuel fragments of small size during the expansion process.

The physical processes that may occur during this initial expansion stage will be discussed in greater detail and parametric models will be outlined for use in source term calculations. Some of the inputs to these models will be based on analyses that have been performed at the University of Virginia, the Argonne National Laboratory and elsewhere.

3.2.2 Description of Expansion Through the Structure

The disassembled core will be assumed to start out at some initial state (1), as shown in Figure 7. This initial state consists of:

a. The masses of fuel, sodium, stainless steel, and fission products; M_{1f}, M_{1s}, M_{1ss}, M_{1fp} respectively.

b. The initial energy states E_1 of each of these components.

The actual core can be expected to have distributed initial properties. Calculations will be performed assuming average states or treating distinct distributed states independently.

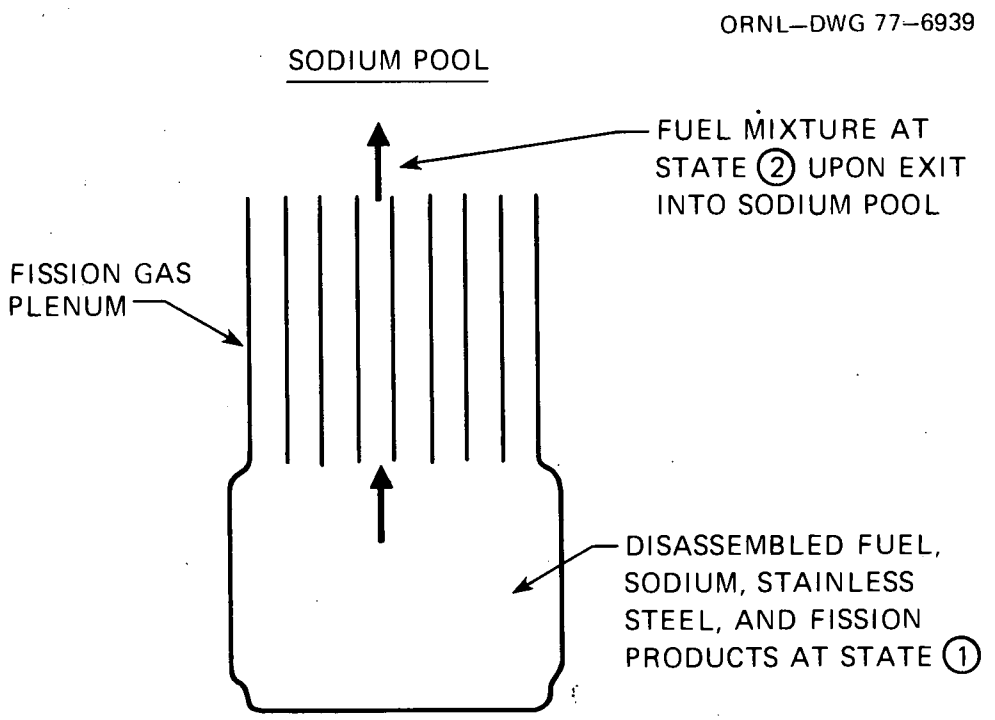

Fig. 7. Initial state of the disassembled core.

The amount of sodium in the core and upper structure before fuel mixture expansion will be dependent on the history of the accident leading to disassembly. In the case of the transient over-power (TOP) accident without scram, sodium remains in the core during disassembly of fuel elements. For a loss of flow (LOF) accident without scram, sodium will void selectively from the central fuel channels outwardly (perhaps leaving a thin film behind), with the limiting case being a core completely empty of sodium upon disassembly. It appears necessary to investigate not only these "limiting" cases, but also intermediate cases treating the initial mass of sodium in the core as a parameter of the model.

The expanding material that becomes a vapor bubble may be mainly sodium, mainly fuel, or some mixture of the two. For significant sodium vaporization to occur, there must be an efficient mixing of sodium and fuel[1] to provide the large heat transfer area needed to permit significant exchange of energy from the fuel to sodium.

If the sodium and fuel are well-mixed, sodium vaporization rates can be large, with possible accompanying fragmentation of fuel (Fig. 8). This may result in a sodium bubble with small fuel drops suspended in it. In the case of simple fuel expansion, (i.e. without fuel coolant interaction) a large amount of fuel vapor may be formed - estimates are of the order of 8 per cent of the initial fuel mass, assuming isentropic expansion[2]. Fuel vapor production by rapid vaporization or "flashing", may result in additional fuel of transportable size that is suspended in the fuel vapor bubble.

While entrainment and fragmentation may increase the particulates in the vapor bubble, heat losses to the "cold" upper structure can reduce the amounts of fuel and sodium vapor. There may be enough heat transferred to the steel clad to cause it to melt while fuel and/or sodium condenses.

The constraining effect of structure on the expansion process may also be important in determining the character of the bubble. Rather than a spherical expansion of fuel and sodium occurring, this mixture may be constrained to jet out of the fission gas plenum zone into the sodium pool. The velocity of the jet exiting the plenum may affect the

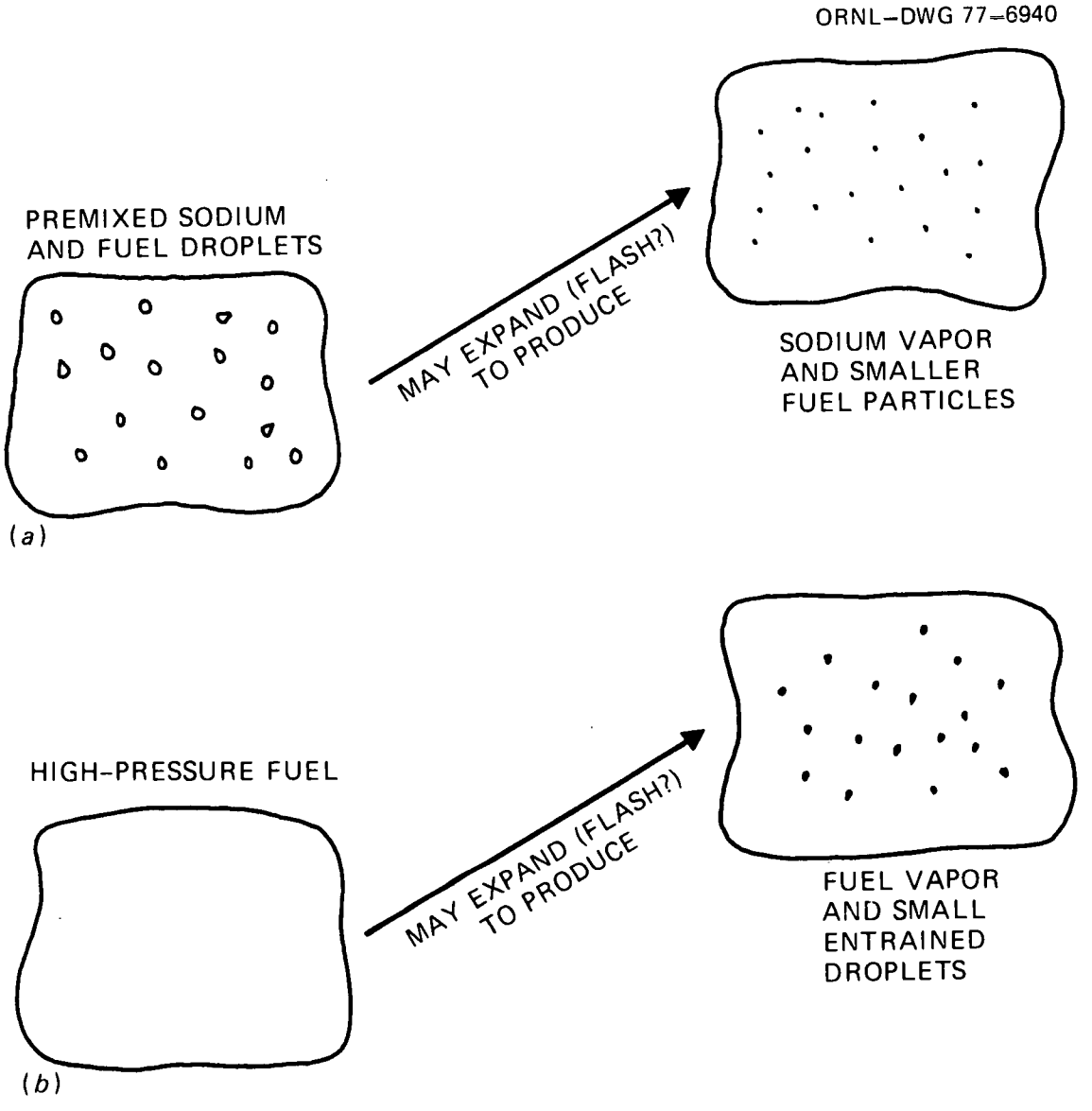

Fig. 8. (a) Sodium expansion, fuel breakup and entrainment;
(b) Fuel expansion, fuel breakup and entrainment.

rate of entrainment of sodium from the sodium pool into the vapor bubble and set up internal circulation patterns that affect subsequent heat transfer and transport of particulates. This entrained sodium can be a heat sink, causing the vapor bubble to condense more rapidly during its subsequent rise through the sodium pool.

3.2.3 Previous Work

Previous work related to fuel mixture expansion through the upper structure can be divided into two areas: studies related to fuel-coolant interaction (FCI), and analyses of heat losses to the fission gas plenum region. Previous work, when applicable, will be used as "input" to the source term calculation, as described in the next section.

At present, fuel-coolant interaction models are parametric and results obtained from experiments have not been well predicted. Padilla[3] presents an excellent review of some of relevant theories. Models that describe the expansion of heated sodium are divided into "thermodynamic" (time independent) and "finite heat transfer rate" models. Rate-limited models are of primary interest because heat transfer and expansion rates are important in determining fuel fragmentation and entrainment effects. The rate model that has been in most use recently is the ANL rate-limited FCI model[4-6]. Large peak sodium pressures are predicted for very short fuel-sodium mixing times and mixed fuel droplet sizes of the order of 100μ. However, dropping experiments of UO_2 in sodium[7] and many of the TREAT meltdown tests[8] with UO_2 and sodium have shown relatively minor pressure generation.

Analyses of heat loss to cold structure indicate a significant potential for cooling and condensing of the hot fuel mixture. In some of this work, sodium is the expanding fluid;[9-11] in others, fuel is the working fluid[12-15]. Much of the analysis assuming fuel condensation also includes effects of the steel structure. Another phenomenon that may be important is the choking of the flow through the fission gas plenum region[16]. This could affect bubble expansion rates and time available for condensation of materials in the upper core structure.

Experiments relevant to structural heat losses have been performed at Stanford Research Institute[17], where high pressure, high temperature steam was expanded through a simulated CRBR upper core. Peak pressures were 22.5% less than those produced when the expansion was performed without simulated structure above the core.

3.2.4 Analysis Plan

Estimates are needed of the state of the fuel mixture as it leaves the fission gas plenum. This "final" state consists of the fuel mixture energy state, velocity, and size of particles transported in the expanding mixture.

The fuel mixture initial state is an input to these calculations. The energy lost from fuel to sodium will be a parameter, and peak fuel mixture pressures will be estimated using current FCI models. From these peak pressures, expansion rates through the upper structure will be found, and these rates related to fragmentation parameters to determine the size of fuel fragments produced (section 3.1).

Current models for heat loss from expanding fuel or sodium to structure will be used to find the amount of heat transferred to structure during the transit time of the fuel mixture expansion through the fission gas plenum. This transit time may be determined by assuming that choked flow occurs, or by estimating it from the fuel mixture expansion rate. It also may be important to estimate the effect of noncondensables on the heat loss from expanding fuel.

3.2.5 References

1. J. Graham, "Molten-Fuel-Coolant Interactions in LMFBR Safety", Trans. Am. Nucl. Soc., 15, 313 (1972)
2. A. B. Reynolds, C. A. Erdman, M. Kirbiyik, "Fuel Vapor Generation in LMFBR Core Disruptive Accidents", Nucl. Technol., 26, 165 (1975)
3. A. Padilla, Jr., "Analysis of Mechanical Work Energy for LMFBR Maximum Accidents", Nucl. Technol., 12, 348 (1971)
4. D. H. Cho, R. O. Ivins, R. W. Wright, A Rate-Limited Model of Molten-Fuel/Coolant Interactions: Model Development and Preliminary Calculations, ANL-7919, Argonne National Laboratory, March 1972.
5. D. H. Cho, R. W. Wright, "A Rate-Limited Model of Molten Fuel-Coolant Interactions", Trans. Am. Nucl. Soc., 13, 659 (1970)
6. D. H. Cho, "Modeling of Molten-Fuel-Coolant Interactions", Trans. Am. Nucl. Soc., 15, 314 (1972)
7. D. R. Armstrong, F. J. Testa, D. C. Raridon, Interaction of Sodium With Molten UO_2 and Stainless Steel Using a Dropping Mode of Contact, ANL-7890, Argonne National Laboratory, Dec. 1971
8. R. W. Wright, et. al., "Summary of Autoclave TREAT Tests on Molten Fuel-Coolant Interactions", in Proceedings of ANS Conference on Fast Reactor Safety, Los Angeles, Apr. 2-4, 1974, Conf-740401-P1, 254 (1974)
9. T. G. Theofonous, H. K. Fauske, "An Energy-Dissipation Mechanism Due to the Cladding of the Fission - Gas Plenum During an HCDA", Trans. Am. Nucl. Soc., 16, 195 (1973)
10. W. L. Chen, "Heat Loss to Cold Structure During an LMFBR Hypothetical Core-Disruptive Accident", Nucl. Technol., 25, 491 (1975)
11. W. L. Chen, D. H. Cho, "Heat Loss to Cold Structure During a Fuel Coolant Interaction", Trans. Am. Nucl. Soc., 17, 353 (1973)
12. D. H. Cho, M. Epstein, "Laminar Film Condensation of Flowing Vapor on a Horizontal Melting Surface", Int. J. Heat Mass Transfer, 20, 23 (1977)
13. D. H. Cho, M. Epstein, "Melting of Steel Structure By Flowing Fuel or Steel Vapor", Trans. Am. Nucl. Soc., 22, 386 (1975)

14. D. H. Cho, "Melting Rates for the Attack of Steel Structure by UO_2 Fuel or Steel Vapor", Trans. Am. Nucl. Soc., 21, 311 (1975)

15. A. B. Reynolds, et. al., Bubble Behavior in LMFBR Core Disruptive Accidents, University of Virginia Annual Report, June 1, 1975 - June 30, 1976, NUREG-0114 (Sept. 1976)

16. Radiological Assessment Models, Seventh Quarterly Report, March-May 1976, General Electric Fast Breeder Reactor Department, June 1976 (GEAP-14034-7)

17. D. W. Ploeger, D. J. Cagliostro, A. L. Florence, Experimental Study of Heat Transfer From a Simulated Hypothetical Core Disruptive Accident Bubble, Stanford Research Institute Report, Project PYU-3929 (Nov. 1975)

3.3 Expansion of the Core Bubble Just After Disassembly

3.3.1 Time-Independent Expansion Thermodynamics (H. W. Bertini)

3.3.1.1 Introduction As part of the evaluation of initial fuel aerosol formation, it is necessary to characterize the core bubble - its size, fuel vapor density, fuel quality, pressure, and temperature - as a starting point for further analyses which examine the bubble's transport behavior as it rises through the sodium pool.

A time-independent thermodynamic approach can be used to make conservative estimates of those characteristics that might exist immediately above the core following a severe hypothetical core disruptive accident. It will be assumed that the properties of the bubble will be established before the bubble rises appreciably, and hence the calculation described in this section will not include effects that result from the rise of the bubble.

The approach will be tailored to scope the values of the quantities of interest as a function of the initial condition which will be taken as a parameter.

For the case of no sodium interaction with the fuel, calculations for free adiabatic expansion (no work) as well as isentropic expansions will be carried out. The results from the adiabatic expansion with no work will give upper limit values for the bubble size and quality. The isentropic expansion calculations will give results that are expected to be closer to the actual situation because the full measure of the work required for the expansion must be extracted from the initial internal energy. However, in the actual case processes may take place, such as thermal losses to structure, which will reduce the energy available for vaporization. These processes will not be included in the isentropic calculation and hence the results will not necessarily represent minimum values.

When it is desired to include specific quantities of sodium to interact with the fuel, the appropriate scoping calculations are not so apparent. The effects of the thermal exchange in reducing the potential for free vapor production should depend on the extent, timing, and nature

of the mixing process. These are difficult to include on a time-independent basis. Appropriate thermodynamic relations can be developed for bounding effects that should provide guidance and insight for comparison with experimental results.

3.3.1.2 Related Work: Most of the existing work on the expansion of the fuel including thermal exchanges with the sodium has been done with time-dependent computer code models. Some of the existing computer codes and previous analytical approaches to the bubble characteristics will be briefly discussed.

The REXCO-HT code[1] and its predecessors[2] were developed to determine the shocks and stresses to the primary containment vessel which might result from an accident. The initial condition of the core must be estimated, i.e., the temperatures and pressures must be supplied as input, and they are usually obtained by homogenizing the output from a VENUS-II calculation. The REXCO-HT code then calculates the progress of the bubble expansion and the shock and pressure waves as a hydrodynamic problem. This procedure while it may be adequate for the intended purposes of the calculation, does not necessarily supply information pertinent to bubble transport of radionuclides.

The FEXPAN code[3,4] uses time-dependent expansion calculations employing Lagrangian coordinates. Initial condition for each mesh cell in the core at the end of disassembly are obtianed from VENUS-II calculations. Spherical, one-dimensional hydrodynamic expansion of the core is calculated in short time steps assuming that the medium is a homogeneous fluid, the expansion is adiabatic, and that thermodynamic equilibrium exists at each time step. Reference 4 includes, for comparison, a time-independent calculation in which each initial cell of the mesh is allowed to expand isentropically and independent to a final pressure. In neither case was the effect of the vaporization of sodium on the characteristics of the bubble included.

The SIMMER code[5] being developed at Los Alamos should have the capability to calculate the fuel vapor density of the bubble with and without sodium. However, this code is large and developmental and its existence should not obviate the need to calculate the maximum values of the bubble characteristics in a simpler fashion.

The last approach to be cited, Hicks and Menzies,[6] is time independent. They estimated the work potential of the sodium vapor in the adiabatic expansion of an intimate mixture of sodium and liquid fuel, but no information on the fuel vapor density is available from this work.

3.3.1.3 Work Plan A brief outline of the approach to be used is given in this section. The method is applicable to that portion of the fuel that is in the saturated liquid state following disassembly. It is this portion of the fuel that, upon flashing, will substantially change the quality from that at the end of disassembly.

Calculations will be carried out for both adiabatic (no work) and adiabatic-isentropic expansions without sodium. Then analogous calculations will be made for mixtures of sodium and fuel. The initial temperatures of the fuel, as well as the final pressure, will be taken as parameters.

For the adiabatic free expansion (no work done) of fuel the quality of the fuel in the final state is given by

$$u_\ell \left(T_i\right) = u_\ell \left(T_f\right) + X\, u_{\ell g} \left(T_f\right) \tag{1}$$

where T_i and T_f are the initial and final temperatures, X is the quality, and u_ℓ and $u_{\ell g}$ are the specific internal energies of the saturated liquid and the difference in internal energy between the saturated vapor and liquid. The equations of state necessary for the calculation are given in Ref. 3

Similarly, for an isentropic expansion to some final pressure, the governing equation involving specific entropy and quality is

$$s_\ell \left(T_i\right) = s_\ell \left(T_f\right) + X\, s_{\ell g} \left(T_f\right) \tag{2}$$

Expressions for the specific internal energy and entropy in the saturated liquid state are also given in Ref. 3. Expressions for $u_{\ell g}$ and $s_{\ell g}$ can be derived from standard thermodynamic relationships in conjunction with the Clausius-Clapeyron equation.

The analogous expressions are more complicated when sodium is included in the calculation. The maximum reduction of fuel vapor would seem to result if the selected quantity of sodium is calculated to reach temperature equilibrium with the fuel before any substantial expansion occurs. At the high thermal state before expansion, the sodium could remove the maximum amount of energy from the fuel which would be at the expense of potential fuel vapor production that would occur during the subsequent (isentropic?) expansion of the fuel.

A "minimum" effect for complete thermal exchange with a given amount of sodium might be bounded if the fuel is calculated to first expand adiabatically to the end state where the fuel temperature is substantially lower, and then interact with the sodium to reach a new equilibrium condition.

Intermediate effects can be included by modelling the process over small expansion intervals allowing specified fractions of the total sodium to interact to equilibrium during each increment of the expansion. Such intermediate calculations would only serve to estimate the rate of energy exchange between the fuel and sodium when compared to actual measurements of the final fuel vapor quality and content of sodium vapor.

3.3.1.4 Results to be Obtained: The results from the calculation will be in parametric form and will be given for various initial and final states, i.e., for the expansion to each assumed final pressure from an initial saturation temperature of the fuel, the characteristics of the bubble (final diameter, fuel vapor density and quality) will be calculated for varying masses of sodium for bounding conditions. The effect of varying the initial temperature of the sodium can be included, and the initial fuel temperature and final pressure will be varied.

In the case of an HCDA in which the various regions of the core are in different states following disassembly, an estimate of the final bubble characteristics can then be readily obtained by superimposing the results from the expansions of each core region where the expansions of each region are taken to be independent of each other. This is equivalent to assuming that there is no mixing between regions during the expansion and should yield the maximum quality.

As discussed above, the isentropic calculations will yield results expected to be more realistic but will not necessarily represent minimum values of fuel vapor quality and bubble size. Differences between results from the adiabatic and isentropic calculations will be of value in estimating values where energies greater than those accounted for in the isentropic expansions are taken from the internal energy of the system.

3.3.1.5 References

1. J. C. Bratis, T. J. Marciniak, and J. Gvildys, REXCO-HT: A Hydrodynamic Containment Code Including Molten-Fuel-Coolant Interactions, ANL-75-15, February 1975
2. Yao-Wen Chang, Joseph Gvildys, and Stanley H. Fistedis, Two-Dimensional Hydrodynamics Analysis for Primary Containment, ANL-7498, November 1969, and reference cited therein.
3. M. Kirbiyik, P. L. Garner, J. G. Refling, and A. B. Reynolds, "Hydrodynamics of Post-Disassembly Fuel Expansion," Nucl. Eng. and Design 35, 441 (1975)
4. A. B. Reynolds and S. R. Rao, Analytical and Planning Assistance for HNL Bubble-Behavior Experiments, ORNL-SUB-3980-1, Aug. 1975
5. C. R. Bell, P. B. Bleiweis, J. E. Boudreau, F. R. Parker, and L. L. Smith, SIMMER-1: An S_n Implicit Multifield, Multicomponent, Eulerian, Recriticality Code for LMFBR Core Disruptive Analysis, LA-NUREG-6467-MS (Draft)
6. E. P. Hicks and D. C. Menzies, Theoretical Studies on the Fast Reactor Maximum Accident, ANL-7120, p. 654, Oct. 11-14, 1965

3.3.2 Time Dependent Expansion Following Disassembly (H. W. Bertini and J. S. White)

3.3.2.1 Introduction

Following disassembly shutdown, the high pressure, high temperature molten regions of the core are presumed to further expand against the structural constraints and against the sodium inertia to form the HCDA bubble at the exit region of the core. The mechanics of formation of this bubble are uncertain. The core material may be ejected upwardly through the upper regions of the core as a two-phase mixture in choked flow to flash and grow as a vapor bubble in the sodium pool. The pressure drop between the core melt region and the expanding bubble may be very high, contributing to the choked flow condition. The "jet" of material leaving the core region may enter the bubble at high velocity inducing strong internal circulation rates which, coupled with the expanding interface, can lead to entrainment of large amounts of the surrounding cooler sodium. The entrainment of this cooler sodium (quantity and droplet sizes) and the establishment of internal circulation as a result of the time dependent expansion processes are believed to be of much importance to the subsequent thermal behavior of the bubble as it moves through the sodium pool. Consequently, as an initial step in examining the entrainment as well as in support of the FAST experiments, we are examining the rates of bubble expansion, the interface velocity, and the magnitude of internal circulation.

3.3.2.2 Related Work

The growth and collapse of bubbles under bodies of liquids have been examined by many authors. An incompressible liquid, Rayleigh type equation[1] ($\ddot{R} = (P - P_\infty)/R\rho - 3\dot{R}^2/2R$), often serves as the basic formulation in which appropriate choices must be made for the variation of the driving potential, $(P - P_\infty)$, as it relates to the thermal conditions, bubble source material, equations-of-state, and dimensional changes.[2,3,4,5]

Safety assessment codes[6,7] have also been developed that treat the extended expansion phases of the HCDA. These rely on numerical solutions, for confined regions, of what are basically the compressible

forms of the momentum and continuity equations on which the Rayleigh equation is based. Of these, only SIMMER[7] appears to have the potential of examining entrainment processes, internal circulation, and internal energy exchange.

3.3.2.3 Work Plan

An attempt will be made to avoid the use of elaborate computer codes in trying to relate the expansion kinetics, the entrainment, and internal circulation to each other. The approach would be based on some form of the incompressible Rayleigh Equation, in which the driving potential, $(P - P_\infty)$, will be developed through consideration of the equation-of-state for fuel, the feed rate out of the core, and equilibrium thermodynamics. The complexity increases in trying to include multi-constituents in the bubble, internal energy exchanges between fuel and coolant, and energy losses to the surroundings. If appropriate formulations can be developed, these effects will be included in parametric fashion.

3.3.2.4 References

1. Lord Rayleigh, Phil, Mag. 34 94 (1917).
2. Robert H. Cole, Underwater Explosions, p. 272 (Princeton University Press 1948)
3. P. L. Garner and C. A. Erdman, Bubble Behavior in LMFBR Core Disruptive Accidents, p. 39, University of Virginia Annual Report June 1, 1975 - June 30, 1976, NUREG-0114.
4. A. B. Reynolds and S. P. Rao, Analytical and Planning Assistance of for HNL Bubble Behavior Experiments, ORNL-SUB-3980-1. University of Virginia Report No. NE-4721-101-75 (Aug. 1975)
5. L. W. Florschuetz and B. T. Chao, Journal of Heat Transfer 87C, 209 (1965).
6. J. C. Bratis, et al., REXCO-HT: A Hydrodynamic Containment Code Including Molten-Fuel-Coolant Interaction, ANL-75-15, (Feb. 1975).
7. C. R. Bell Et al., SIMMER-I: An S_n Implicit, Multifield, Multicomponent, Eulerian, Recriticality Code for LMFBR Disrupted Core Analysis, LA-NUREG-6467-MS (Draft).

3.4 Thermal Effects as the Bubble Rises Through the Sodium Pool

T. S. Kress, M. N. Ozisik*

3.4.1 Introduction

This section addresses the phase of an HCDA immediately following the initial expansion of fuel vapor (and/or sodium vapor) which is assummed to have created a bubble (or bubbles) at the exit section of the fission gas plenum region. The composition of this bubble is uncertain but is assumed to be at a much higher temperature than the surrounding sodium pool and should rise toward the cover gas region by buoyancy. As the bubble moves through the sodium, this higher temperature will provide the potential for thermal exchange with the sodium and with other heat sinks.

The objective of the thermal modeling of this phase of the HCDA is to determine the quantities and states of potential source material (fuel and fission products) that survive the transport to the cover-gas region. This will serve as a basis for determining the effects of the thermal exchange on the characteristics of the material that may subsequently be released from the head region into the secondary containment.

Only two thermal analyses[1,2] are known to exist that are aimed directly at this phase of the HCDA. Theophanous and Fauske[1] considered the bubble as being made up of sodium vapor. They treated heat and mass transfer as a purely diffusional process and approximated the bubble in a semi-infinite domain. They included the effects of non-condensable gases and applied a similarity analysis to solve the resulting coupled mass and heat transfer differential equations. Reynolds, Kennedy, and Honig[2] also assumed a sodium vapor bubble with slab geometry. They treated heat transfer on the liquid side as a purely diffusional process, assigned a condensation heat transfer coefficient for condensation onto the liquid-vapor interface and solved the resulting equations numerically. New works in progress include that being done at ORNL in the ART program, additional work at the University of Virginia[3], at Los Alamos Scientific Laboratory in the SIMMER program[4], and the ERDA sponsored source attenuation work of General Electric[5].

*North Carolina State University, Consultant to ART Program

Experimental data for these conditions are practically non-existent. The observations at Stanford Research Institute[6] (SRI), in which explosive mixtures were used to investigate the behavior of small scale, HCDA-like bubbles under water, have revealed that the expansion process may establish considerable internal circulation that, along with the expansion itself, appears to lead to entrainment of large amounts of the surrounding liquid as droplets. In view of this, it appears that entrained sodium droplets should be considered as a possible heat sink in addition to the interface itself and any internal structure in the path of the bubble. Furthermore, if strong circulation rates do exist, as observed in the SRI experiments, these can greatly enhance the thermal exchanges and, should also be considered in analyses of this phase of the HCDA. It is still an open question whether the composition of the initial bubble is primarily fuel vapor or sodium vapor.

An exact heat and mass transfer analysis of all the thermal phenomena occurring in an HCDA bubble would be complicated, requiring perhaps a large computerized model. Such an approach would not be appropriate in the ART program for purposes of source attenuation evaluation for it is not clear that increased model complexity will necessarily result in a more accurate description of the overall behavior. Rather, simplifying assumptions that reduce the models to forms amenable to direct analysis seem called for. With this view in mind, then, the following models under development in the ART program represent what we feel is an effective approach to source attenuation thermal modeling.

3.4.2 Proposed Simplified Thermal Model

In the following thermal model, an arbitrary HCDA bubble is considered that consists of some definite but unspecified quantity of fuel vapor, sodium vapor, entrained sodium droplets, internal surface, and non-condensable fission gases. It will be assumed that sufficient internal (in the bubble) and external (in the sodium) circulation exists that heat and mass transfer can be described as being governed by turbulent convection (although radiant heat transfer from the vapor phase to the interface may also be important).

Three heat sinks will be assumed to exist: internal structure covered by a thin liquid sodium film, entrained sodium droplets, and the bubble interface itself. The heat transfer processes will be characterized by the simple use of appropriate condensation heat transfer coefficients. It is intended that separate models be developed to determine the values for the different coefficients for the three heat sinks. Consequently, the basic phenomenological equation in this model is:

$$\dot{m}_i = \frac{h_i \Delta T_i}{H_{fg}} \qquad i = 1,2,3 \tag{1}$$

where $\dot{m}_i$ are the condensation mass fluxes,

($\dot{m}_1$ = flux to the bubble interface

$\dot{m}_2$ = flux to internal surface

$\dot{m}_3$ = flux to entrained droplets)

ΔT_i are the temperature potentials

h_i are the heat transfer coefficients

and H_{fg} is the latent heat of condensation for the vapor.

A mass balance for the conservation of condensable vapor may be stated as

$$\begin{bmatrix}\text{Total rate of loss of}\\ \text{vapor from the bubble}\end{bmatrix} = \begin{bmatrix}\text{Rate of condensation due to heat trans-}\\ \text{fer to the liquid-vapor interface}\end{bmatrix} +$$

$$\begin{bmatrix}\text{Rate of condensation}\\ \text{on internal surface}\end{bmatrix} + \begin{bmatrix}\text{Rate of condensation on}\\ \text{entrained sodium droplets}\end{bmatrix} .$$

In terms of the assumed phenomenological equation, (Eq. 1), this becomes

$$\frac{-dM_v(t)}{dt} = A(t)\dot{m}_b + \alpha_s A_o \dot{m}_s + \alpha_d A_o \dot{m}_d \tag{2}$$

Where $M_v(t)$ = total mass of vapor in the bubble at time t

$A(t)$ = surface area of the liquid-vapor interface at time t

A_o = surface area of the liquid-vapor interface at t=o

α_s = the ratio, (internal surface area)/A_o

α_d = the ratio, (surface area of entrained droplets)/A_o

The above simplified model, Eq. (2), is arbitrary in the sense that appropriate values must be provided for the surface areas, for the individual transfer coefficients and for the temperature potentials for each heat sink. Further, in the actual solution of the equations which

arise out of (2), only the liquid-vapor interface surface area A(t) is allowed to vary with time, while time changes in internal and entrained droplet areas are assumed negligible.

3.4.2.1 Temperature Potentials. The temperature differences between the condensable fuel vapor and the three heat sinks will vary over the bubble rise period (estimated to be of the order of 1-2 seconds). Therefore, to permit easy solution of Equation (2), it will be assumed that appropriate average values can be used for each temperature difference and for each heat transfer coefficient.

Consider, first, the mean temperature difference between the vapor and the bubble interface itself. The maximum value that this temperature difference could have is the difference between the initial bubble vapor temperature, T_v, and the initial bulk sodium temperature, T_L. However, if there is sufficient time to approach a steady state, a heat balance would give

$$h_L \left(T_b - T_L\right) = h_b \left(T_v - T_b\right)$$

where h_b = an average condensation heat transfer coefficient on the vapor side

h_L = an average liquid side heat transfer coefficient

T_b = the interface temperature

T_L = the bulk liquid sodium temperature

and T_v = the condensable vapor temperature.

Consequently,

$$\Delta T_b = \left(T_v - T_b\right) = \frac{h_L}{h_L + h_b} \left(T_v - T_L\right) = C_b \left(T_v - T_L\right) \qquad (3)$$

Equation (3), perhaps, represents the minimum value for the interface temperature potential. It would appear to be an appropriate value to use for the averaged temperature potential where average values are to be used for h_L and h_b. Similarly, such considerations appear appropriate for the temperature potentials for the internal surface and for entrained sodium droplets, so that we have:

$$\Delta T_s \cong \left(T_v - T_L\right) C_s$$

and

$$\Delta T_d \cong \left(T_v - T_L\right) C_d$$

where $C_s = \dfrac{h_s}{h_{1s} + h_s}$ and $C_d = \dfrac{h_d}{h_{1d} + h_d}$

h_{1d} and h_{1s} are averaged coefficients that include the thermal responses for the droplets and the structure on the respective liquid sides. With the above simplifications, the basic mass balance equation (2) becomes

$$\frac{dF(t)}{dt} = -\frac{A_o}{H_{fg} M_{vo}} \left\{ \frac{A(t)}{A_o} h_b C_b \left(T_v - T_L\right) + \alpha_s h_s C_s \left(T_v - T_L\right) + \alpha_d h_d C_d \left(T_v - T_L\right) \right\} \quad (4)$$

where F(t) is the fraction of condensable vapor left in the bubble at any time, $M_v(t)/M_{vo}$.

Assuming a spherical bubble, we have

$$\frac{A(t)}{A_o} = \left[\frac{V(t)}{V_o}\right]^{2/3}. \quad (5)$$

Various equations-of-state can be used to establish the relationship between V(t) and V_o. For simplicity in the present analysis it is assumed that the vapor-gas mixture inside the bubble behaves as a perfect gas and that the total pressure and temperature remains constant during the rise. Therefore,

$$V(t)/V_o = \left(M_g + M_v(t)\right) / \left(M_g + M_{vo}\right) = \left(X_g + F(t)\right) / \left(X_g + 1\right) \quad (6)$$

where M_g = the mass of non-condensable gases present in the bubble
and X_g = the ratio, $\left(M_g/M_{vo}\right)$.

Substituting (5) and (6) into (4) and combining the coefficients

$$\alpha_s C_s \equiv \beta_s$$

$$\alpha_d C_d \equiv \beta_d$$

gives for the final simplified model mass balance equation

$$\frac{dF(t)}{dt} = \frac{-A_o h_b \left(T_v - T_L\right)}{H_{fg} M_{vo}} \left\{ \left[\frac{X_g + F(t)}{X_g + 1}\right]^{2/3} C_b + \frac{\beta_s h_s + \beta_d h_d}{h_b} \right\}. \quad (7)$$

Equation (7) should lend itself to easy solution on a computer to determine the fraction of vapor, F(t), surviving the rise through the sodium.

3.4.2.2 Heat Transfer Coefficients. To apply the simplified model presented above, additional modeling will be required to develop appropriate values to use for the various coefficients β_s, β_d, h_L, h_b, h_s, and h_d. The development of these coefficients will also be a part of the thermal modeling effort. In addition, it is believed that the portion of the ART experimental program designated FAST[7] (the under sodium bubble transport experiments) will be valuable in establishing empirical values for the coefficients and in validating the simplified thermal model itself.

The coefficients β_s and h_s relate to the amount of internal structural surface encountered by the bubble and its thermal response over a short time period. The coefficients β_d and h_d involve the response of entrained sodium droplets and will require droplet sizes and entrainment rates.

Of the remaining coefficients, perhaps the most difficult one to establish is h_b, the coefficient for turbulent convective condensation of fuel vapor onto the bubble interface in the presence of non-condensable fission gases. The type of analysis discussed below can be used to establish both h_L and h_b (not including the effects of radiant heat transfer).

The condensation of a large sodium HCDA vapor bubble containing non-condensable fission gases has been analyzed by Theophanus and Fauske.[1] Their analysis, however, was for condensing sodium vapor under conditions in which molecular conduction and diffusion were dominant. A preliminary estimate has indicated that internal circulation in a HCDA bubble is likely to be turbulent. Consequently, a boundary-layer type analysis will be made, similar to that of Ref. 1, but which includes the effects of turbulence.

Consider a plane interface having relatively cool sodium on one side and a mixture of hot fuel vapor and noncondensable fission gases on the other (see Fig. 9).

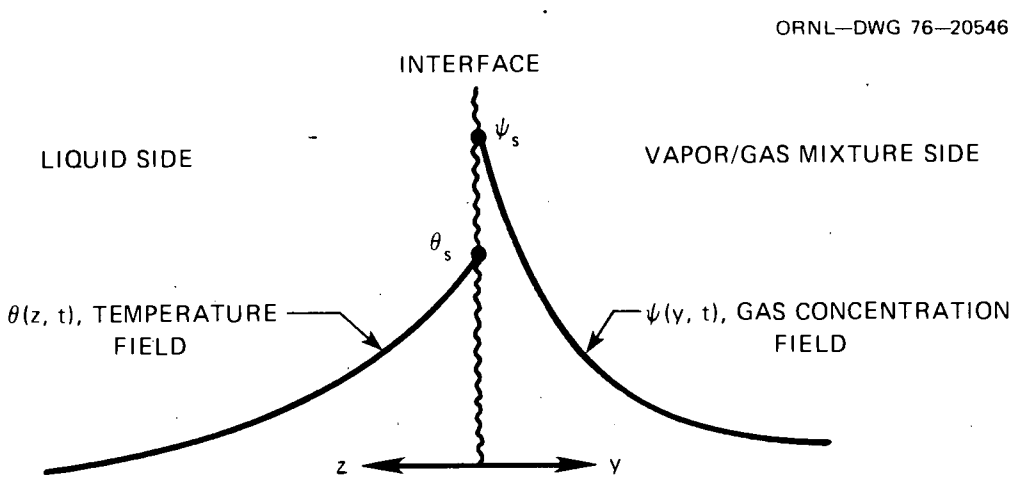

Fig. 9. Temperature and concentration fields at the interface of an HCDA bubble.

The appropriate turbulent equations that describe the temperature field in the liquid and the noncondensable gas concentration field are given below.

On the liquid side, the temperature field is governed by

$$\frac{\partial\theta(z,t)}{\partial t} \quad \frac{\partial}{\partial z}\left[\alpha^*(z)\ \frac{\partial\theta}{\partial z}\right], \tag{8}$$

where $\theta \equiv \left(T - T_L\right)$,

$= \theta_s$ at $z = 0$,

$= 0$ at $z \to \infty$,

$= 0$ for $t = 0$,

$\alpha^*(z) \equiv \alpha + \frac{1}{Pr_t}\ \varepsilon_h(z)$,

in which α is the molecular thermal diffusivity, $\varepsilon_h(z)$ is a turbulent eddy diffusivity for heat transfer that is some unspecified function of position, and Pr_t is the turbulent Prandtl number.

On the gas-vapor side, the concentration of noncondensables is described by

$$\frac{\partial\psi(y,t)}{\partial t} + \left(\frac{D}{\Psi_s + X_\infty}\ \frac{\partial\psi}{\partial y}\bigg|_{y=0}\right)\frac{\partial\psi}{\partial y} = \frac{\partial}{\partial y}\left[D^*(y)\ \frac{\partial\psi}{\partial y}\right], \tag{9}$$

where $\psi \equiv \left(X - X_\infty\right)$

$= \psi_s$ at $y = 0$,

$= 0$ as $y \to \infty$,

$= 0$ at $t = 0$,

$D^*(y) \equiv D + \frac{1}{Sc_t}\ \varepsilon_m(y)$,

in which D is the molecular coefficient for diffusion of the gas, $\varepsilon_m(y)$ is a turbulent eddy diffusion coefficient for mass transfer that is also a function of position, and Sc_t is the turbulent Schmidt number.

The implementation of the above model equations requires functions for the eddy coefficients as well as for the turbulent Prandtl and Schmidt number.

Suitable models for these parameters are being selected to include the effects of the flux of condensing vapors and the internal and external velocity patterns. Then, using appropriate boundary conditions and state equations, the turbulent condensation model can be solved numerically

to determine the temperature field, the concentration field, the condensation rates, and average values for heat and mass transfer coefficients over some specified short time period. The averaged values developed h_L and h_b can be used directly in the simplified model represented by Equation (7).

3.4.2.3 Effects of Radiant Heat Transfer. If the HCDA bubble is composed chiefly of fuel vapor, its temperature is likely to be in excess of 4000°K where radiation heat transfer can be quite effective for condensing the vapors.

In keeping with the simplified model approach, it is desired to include the effects of radiant heat transfer in an approximate, but representative, manner. Consequently, is assumed that condensation of fuel vapor as a result of radiative heat losses to the sodium interface can be approximated by an equation of the form

$$\dot{m}_r = \frac{\sigma\varepsilon}{H_{fg}} \left(T_v^{\,4} - T_b^{\,4}\right) .$$

If $T_v >> T_b$, this may be further approximated as

$$\dot{m}_r \cong \frac{\sigma\varepsilon}{H_{fg}} \left(T_v^{\,3}\right) \left(T_v - T_b\right)$$

$$\equiv \frac{h_{br}}{H_{fg}} \left(T_v - T_b\right) , \qquad (10)$$

which is identical in form to the basic phenomenological Equation (1). In the case of the HCDA bubble, T_v is not sufficiently greater than T_b to warrant the approximation, $\left(T_v^{\,4} - T_b^{\,4}\right) \cong T_v^{\,3} \left(T_v - T_b\right)$. However, the terms that are neglected in this approximation would increase the effective h_{br} if included. The use of Eq. (10) would be conservative since less fuel vapor condensation will be predicted than if the additional terms are included. In addition Eq. (10) assumes black body conditions. The effective h_{br} will have to be made smaller to account for reflections at the sodium interface where the effective emissivity is uncertain. Consequently more precise treatment of the effects of radiant heat transfer are felt to be unwarranted at this time, and it is believed that radiant heat transfer can be included in the formation of Equation (7) by merely adjusting the value of h_b to include a contribution due to radiation.

3.4.3 Source Considerations Related to Thermal Modeling

The above simplified thermal model is intended to determine the rate of condensation of fuel vapor during the HCDA bubble rise. It has been tacitly assumed that condensed fuel vapor and a proportionate amount of solid fission products are essentially removed from consideration as part of the HCDA source term. There is no real justification for this assumption. It is conceivable that the condensed fuel merely becomes entrapped aerosol to be carried along with the bubble and still may constitute a portion of the source to be released into the secondary containment. The determination of the actual disposition of condensed fuel vapor must rely on experimental observations like those planned in the FAST facility of the ART program.

Consequently, additional modeling may be required to couple the thermal models to aerosol nucleation and attenuation models that will analyze the characteristics and transportability of fuel aerosols within the bubble.

Similar thermal-aerosol models can be applied to the cover-gas space transient if the leakage paths are established to be small enough to provide significant hold-up of the vapors, gases, and aerosols in the cover-gas region before release into the secondary containment. It is apparent that a cover-gas region thermal model can be quite similar to the simplified model developed above for the bubble although the various coefficients may have quite different values and a leakage term would have to be included in the mass balance equation.

3.4.4 References

1. T. G. Theofauous, H. K. Fauske "The Effect of Noncondensibles on the Rate of Sodium-Vapor Condensation from a Single Rising HCDA Bubble," Trans. Am. Nucl. Soc. 15 No. 2. 814 (1972).
2. A. B. Reynolds, M. F. Kennedy, H. Honig "Condensation of a Large Sodium Vapor Bubble After a Fast Reactor Disassembly Accident", Trans. Am. Nucl. Soc. 14 No. 2, 738, (1971).
3. A. B. Reynolds et al. Bubble Behavior in LMFBR Core Disruptive Accidents, Annual Report June 1, 1975-June 30, 1976, University of Virginia, NUREG-0114, September 1976.
4. C. R. Bell et al. SIMMER-1: An S_n... Code for LMFBR Disrupted Core Analysis, LA-NUREG-6467MS, Los Alamos Scientific Laboratory January 1977.
5. Radiological Assessment Models, Fifth Quarterly Report, September-November 1975, GEAP-14034-5, General Electric Company, December 1975.
6. D. J. Cagliostro, et al., Quarterly Progress Report No. 5, 1 January-31 March 1976, Experimental Model Studies of Bubbles Generated in Fast Breeder Reactors During a Hypothetical Core Disruptive Accident, Stanford Research Institute, 23 April 1976.
7. T. S. Kress, G. W. Parker, M. H. Fontana, Work Plan: Transient Release Program, ORNL-TM-4875, Oak Ridge National Laboratory (1975)

3.5 Aerosol Formation and Attenuation in the Rising Bubble and the Cover Gas Region

M. L. Tobias

Once the bubble has been formed and is rising it is important to know to what extent aerosol formation occurs within it and what particle and droplet removal mechanisms there may be. To our knowledge, although the problem has been approached, there exists no explicit treatment in the literature of in-bubble aerosol formation mechanisms. Attenuation information is less limited but still scanty. Epstein and Cho[1] discuss aerosol formation criteria in connection with condensation of steel or UO_2 vapor on subassembly duct walls and also when contacting liquid sodium. Fog formation is predicted in both cases at sufficiently low termperatures at the interface between the vapor and the condensate film. They also point out that radiation heat fluxes are highly significant in the case of a condensing sodium fog at 1100K. Kennedy and Reynolds[2] utilized the size distribution obtained from the UO_2-sodium dropping experiments of Armstrong et al[3] in order to calculate the attenuation of aerosol particles from a rising bubble. It is not clear that the dropping experiment size distribution results are necessarily appropriate to this situation.

Fuchs[4] discusses aerosol attenuation in a rising bubble but offers nothing concerning aerosol formation under such circumstances. He gives simple formulas for inertial, sedimentation and difference deposition. Aside from these, he notes that absorption in bubbling is generally poor, strongly reduced by increasing temperature due to flow of vapor-gas mixture away from the surface.

Once the bubble has penetrated the surface, aerosol should be produced there composed not only of fuel but also of sodium by the film drop and jet drop mechanisms.[5,6,7] Fuel aerosol formation by nucleation from the vapor state should continue and there is some possibility that aerosols might be generated, analogously to ocean aerosols, by evaporation of sodium droplets leaving behind the residue of dissolved material, but nothing has been found concerning this conjecture. In any case the behavior of the aerosol should be calculable by procedures similar to

those used for the secondary containment, making allowances, for the widely different condition of concentration, containment volume temperature, pressure, nucleation and the lack of a chemically active atmosphere.[8]

The work plan for analysis of the mechanism of aerosol generation and attenuation in the rising bubble should consist of the following aspects of the subject:

1. A brief literature review to continue and complete what has been reported here.
2. Development of simple models, related to the thermal models discussed in Section 3.4 to represent conceivable mechanisms.
3. The planning and proposal of experiments based upon these models using the existing experimental facilities.

3.5.1 References

1. M. Epstein, D. H. Cho, "Fog Formation in Hypothetical LMFBR Accidents" Trans. Am. Nucl. Soc. 21 324 (1975); See also Trans. Am. Nucl. Soc. 18 222 (1974)
2. M. F. Kennedy, A. B. Reynolds, "Plutonium Transport to the Secondary Containment in an LMFBR Accident", Trans. Am. Nucl. Soc. 16 196 (1973)
3. D. R. Armstrong, F. G. Testa, and R. Raridon, Jr., "Molten UO_2-Sodium Dropping Experiments", Trans. Am. Nucl. Soc. 13 660 (1970)
4. N. A. Fuchs, The Mechanics of Aerosols, pp. 240-245, The MacMillan Co., New York 1964
5. Milos Tomaides, K. T. Whitby, "Generation of Aerosols by Bursting of Single Bubbles", in Fine Particles, B. Y. H. Liu, Editor, p. 235, Academic Press, New York 1976
6. Garner, F. H., R. M. Ellis, and J. A. Lacey, "The Size Distribution and Entrainment of Droplets", Trans. Inst. Chem Engrs., 32, pp. 222-235 (1954)
7. Blanchard, D. C., "The Electrification of the Atmosphere by Particles from Bubbles in the Sea", Progress In Oceanography, Vol. 1, Mary Sears, Editor, The MacMillan Company (1963)
8. A. B. Reynolds, et al., Bubble Behavior in LMFBR Core Disruptive Accidents, Annual Report June 1, 1975 - June 30, 1976, pp. 86-111 NUREG-0114 Sept. 1976

3.6 Formation and Attenuation of Aerosols as a Result of Containment Leakage

M. L. Tobias

3.6.1 General Remarks

Following a core disruptive accident, it may be supposed that the portion of the core which has vaporized, including fission products and gaseous sodium, rises to the top of the containment vessel and exists there above the sodium at a pressure and temperature that will depend upon the amount of leakage caused by damage to the vessel head. From there it can be imagined to leak for some period of time through an opening of some size into the secondary containment. Two important questions then arise. First, if the opening is small, can plugging occur due to the presence of airborne particulate fuel aerosols or nucleation during passage which would attenuate the release and therefore reduce potential hazard? Second, what are the effects on the aerosol on passing from a high-pressure, high temperature region into a relatively cold, low pressure region? This information is necessary for using computer codes to characterize the behavior of the aerosol in the secondary containment, such as HAARM-2[1] or PARDISEKO[2,3]. These codes require such input as the initial particle number concentration or a source rate, the variance and mean radius of the initial assumed log normal distribution, dynamic and collision form factors, and other properties which would depend on the nature of the material released as a function of time.

3.6.2 Attenuation of Aerosols Due to Plugging

Previous plugging studies, both experimental and analytical, have dealt mainly with phenomena associated with an existing aerosol-gas mixture passing through cracks and fissures in the secondary containment. Nelson et al[4] describe experimental studies[5] at Atomics International which show that leaks through holes as small as 1 mm are quickly plugged by sodium oxide aerosols. The aerosols were generated by sodium pool fires and pressure differentials were $\leq$ 0.68 atmospheres. While considerable qualitative and experimental observations have been made, Nelson

et al. note that no quantitative theory for plug formation is presently available. An earlier review[6] exists however, which deals to some extent with theoretical issues. General Electric analytical work is described in refs. (7,8). Ref. 7 starts with an expression, easily derived from a mass balance relationship,

$$C_o/\bar{C} = \text{Exp}\left(Pv_s\ell/Av\right)$$

Where C_o is the entering particle concentration, $\bar{C}$ is the average leaving concentration from a leak path of constant cross section A, perimeter P, and deposition length ℓ, for a gas stream moving at velocity v. The quantity v_s is the deposition velocity for particles, and it is on this quantity that further analysis concentrates. Factors affecting v_s include gravitational settling, electrostatic scattering, thermal mechanisms, inertial mechanisms (such as the effects of obstacles, bends or obstructions), and adhesion forces. A survey of experimental data on deposition of such aerosols as Al_2O_3, cigarette smoke, sodium oxide[6], iron, and zinc sulfide is also reported for both laminar and turbulent flow. These ideas were implemented in the GALP code, reported in the review by Huang.[8] He observes however that the code embodies a number of "extremely conservative" assumptions, including neglect of aerosol agglomeration, smooth, straight, constant cross section leakage paths, and no entrance plugging. On this basis, he observes that further development is needed to place the attenuation calculation on a more realistic basis. While the review reports a few GALP sample calculations, no mention is made of either an experimental program to test calculational methods, nor is there a discussion of comparisons with such data as given in the survey of ref. 7.

3.6.3 Aerosol Generation During Free Expansion

The literature of aerosol generation emphasizes the formation of monodisperse types for testing purposes,[9,10,11] such as by the Sinclair-LaMer generator. An extensive and rather abstract theoretical discussion is presented by Hidy and Brock[12] and a more empirical treatment is given by Green and Lane[13] for the formation of polydisperse aerosols. However, it is clear that nothing quite like the combined set of circumstances

characteristic of the HCDA is to be found in the literature except in Buttery's review.[14] As might be expected, his study of aerosol production in choked flow is a synthesis of results from related physical phenomena, e.g. use of Hinze's citerion (Sec. 3.1.3.1) for aerodynamic breakup to compute maximum stable drop size. The aerosol resulting from a leak in the primary containment would have many components having a variety of chemical reaction possibilities not only with air but with each other. Obviously, the principal component would be sodium vapor oxidizing rapidly in the air of the secondary containment. There is therefore a relationship with the Atomics International sodium fire studies alluded to earlier[5] but it would seem that only a theoretical program aimed at developing suitable experiments would afford satisfactory information.

3.6.4 Work Plan

The analysis of formation of aerosols through a leak should be continued along the lines which Buttery has indicated. Experimental data from existing and planned sodium spray fire experiments at AI, HEDL, and ORNL will form a valuable, if partial, testing ground for such theories. However, such experiments will offer no direct testing of the behavior of uranium or plutonium oxides under such circumstances nor of the various fission product elements which may offer significant hazard. The analytical program will be directed toward the planning of experiments for these materials.

Aerosol attenuation by plugging deserves particular attention, expecially to determine the opening size beyond which it is unimportant. The ideas in the work described in section 3.6.2 need to be brought together into a conservative calculational scheme in order to create a standard approach. Such a study would naturally reveal areas of uncertainty which would suggest appropriate experiments.

3.6.5 References

1. L. D. Reed and J. A. Gieseke, HAARM-2 Users Manual, BMI-X-665, Oct. 31, 1975, Battelle Columbus Laboratories
2. K. Keller, Aerosol Behavior in Closed Container (PARDISEKO II), EURFNR - 1117 (KFK-1758) (August 1973)
3. H. Jordan and Chr. Sack, PARDISEKO III: A Computer Code for Determining the Behavior of Contained Nuclear Aerosols, EURFNR-1268 (KFK-2151), (May 1975)
4. C. T. Nelson, R. P. Johnson, E. V. Vaughan, C. A. Guderjahn, and H. A. Morewitz, "Some Potential Reductions in the Release of Radioactivity Under LMFBR Accident Conditions", International Meeting on Fast Reactor Safety and Related Physics, Chicago, Ill. Oct. 5-8, 1976.
5. Activity regularly reported as Subtask E-Aerosol Leakage in Quarterly Technical Progress Report, Nuclear Safety, Characterization of Sodium Fires and Fast Reactor Fission Products and corresponding Annual Technical Progress Reports for Government Fiscal Years. A recent example is AI-ERDA-13175
6. C. T. Nelson, Gas and Particulate Leakage, TI-707-130-033, Nov. 13, 1974
7. Radiological Assessment Models, Third Quarterly Report, March-May 1975, GEAP-14034-3, June 1975
8. T. C. Huang, Review and Developments of Aerosol Analytical Methods, GEAP-14147, September 1976
9. Handbook on Aerosols, Chapter 6, United States Atomic Energy Commission, Washington, D. C., 1950, Reissued 1963
10. Morton Corn and Nurtan A. Esmen, "Aerosol Generation", Chapter 2 of Handbook on Aerosols, Richard Dennis, Editor, TID-26608, USERDA, 1976
11. Fuchs, N. A. and Sutugin, A. G., "Generation and Use of Monodisperse Aerosols" Chapter 1 of Aerosol Science C. N. Davies, Editor, Academic Press, 1966
12. G. M. Hidy and J. R. Brock, The Dynamics of Aerocolloidal Systems, Pergamon Press Suc., 1970

13. H. L. Green and W. R. Lane, Chapter 2, Particulate Clouds: Dusts Smokes and Mists, 2nd Edition D. Van Nostrand Company, 1964

14. N. E. Buttery, Possible Aerosol Formation Mechanisms Following LMFBR Whole Core Accidents, RD/B/N3497 (Rev) Central Electricity Generating Board, Research Department, Berkeley Nuclear Laboratories, January 1976

3.7 Aerosol Behavior in the Secondary Containment

L. F. Parsly, Jr.

3.7.1 General Remarks

Any aerosol which exists in the secondary containment is a potential source for leakage to the environment. The source term for subsequent dispersion/dose calculations will therefore depend on calculations of the concentration vs time behavior plus leakage vs time behavior in the secondary containment.

In the case of an HCDA release in the manner described in the previous sections, the aerosol source for the secondary containment consists of fuel, fission products and sodium which have leaked from the cover gas region. The fuel and fission products will be in the form of dispersed particles and gases, while the sodium might be initially in the form of vapor, liquid droplets, or bulk liquid. Each of these forms of sodium will burn in its characteristic way: instantaneously for vapor, as a spray if in the form of droplets, or as a pool if bulk liquid or droplets are too big to burn completely in the atmosphere. The pressure and temperature history of unvented containment buildings will depend to a large extent on the course of the sodium fire.

The aerosol in the containment is a dynamic system. Aerosol particles collide with each other and stick together, due either to Brownian movement or to the larger particles falling faster and overtaking and capturing smaller ones. Thus the number density tends to decrease and the particle size to increase with time. Particles may diffuse to surfaces due to Brownian motion and stick to the surfaces due to van der Waals forces. Where temperature gradients exist, thermophoresis, that is, the net movement of particles down the temperature gradient, occurs. Particles tend to settle on the floor due to gravity. The net result is that the aerosol concentration in any confined space in the absence of a continued source will decrease with time.

A number of computer codes have been written to model both sodium fires and aerosol behavior in containment vessels. Some of these are described below. These existing models will be used and validated with the experimental results. Where appropriate, recommendations for modifications to these models based upon analyses and experiments will be made.

The approach will be to use the appropriate computer codes with suitable input assumptions to predict the course of both sodium fires and aerosol behavior in the ORNL containment vessel experiments, and to compare the results of the experiments with the pre-test predictions. Experiments will be designed to validate the models under mixed aerosol conditions with particular attention to features related to vessel size.[1]

3.7.2 Computer Codes for Secondary Containment Analysis

Computer codes available to describe sodium burning include SOFIRE-II[2], SPRAY-II[3], SOMIX[4] and CACECO[5]. SOFIRE-II calculates sodium burning and associated heat transport effects during pool fires. The model assumes that the rate of burning is controlled by diffusion of oxygen to the sodium surface. The code appears adequate to describe pool fires, except possibly in a case where significant vaporization of sodium form the pool surface occurs.

Sarma et al.[6] report that SOFIRE-II gives good results for pool fire analysis. However, they point out the need for providing good values of the monoxide/peroxide ratio, mass transfer coefficients and emissivity view factors in the input. These parameters can strongly influence the calculated results.

SPRAY-II analyszes sodium spray fires in up to 21% oxygen atmospheres. It uses the assumption that the burning rate is controlled by oxygen diffusion for 4-21% oxygen and by sodium vapor diffusion for 0-4% oxygen. Sarma et al. state that reasonable results are obtained for a non-venting situation.

SOMIX is being developed by Atomics International to calculate convective patterns and pressure and temperature histories in inerted ($\leq$ 2% O_2) spaces in LMFBR power plants. The code is still under development and has not been released.

It is planned to use SOFIRE-II and SPRAY-II separately or in combination to provide sodium fire source term predictions for this study. Alternatively, it may be assumed that sodium leaked into the secondary containment is completely converted to sodium oxide aerosol and treat this as material initially present.

Aerosol analysis codes presently available in this country include HAARM-2, other variations of HAA-3 and PARDISEKO-III. All of these codes undertake to solve an integro-differential equation which describes the behavior of an aerosol in a containment volume. The equation in conceptional form is:

$$
\begin{aligned}
\frac{\partial n(r,t)}{\partial t} &= \left[\frac{\partial n(r,t)}{\partial t}\right] && \text{Brownian Agglomeration} \\
&+ \left[\frac{\partial n(r,t)}{\partial t}\right] && \text{Gravitational Agglomeration} \\
&+ \left[\frac{\partial n(r,t)}{\partial t}\right] && \text{Settling} \\
&+ \left[\frac{\partial n(r,t)}{\partial t}\right] && \text{Plateout} \\
&+ \left[\frac{\partial n(r,t)}{\partial t}\right] && \text{Sources} \\
&+ \left[\frac{\partial n(r,t)}{\partial t}\right] && \text{Leaks} \\
&+ \text{etc.}
\end{aligned}
$$

which must be integrated over the entire size range to describe the dynamics of an aerosol. Obvously such an equation is difficult to solve, and different workers have used various solution techniques.

The approach taken in HAA-3[7] is to take the aerosol particle size distibution to be log-normal distribution, the integro-differential equation is reduced to a system of three ordinary differential equations which are integrated directly by rapid numerical procedures. Brownian and gravitational agglomeration, plating due to Brownian diffusion, settling and leakage are included as possible removal mechanisms; an existing aerosol, a source or both can be treated. Leakage from a primary containment vessel can be used as a log-normal source for a secondary containment calculation. A density correction factor and a boundary layer thickness are input parameters. Of the several variations of HAA-3 which exist, the the HAARM-2[8] will be used. In this code, the density correction factor is treated by a built in formalism originally due to Stober[9]. A thermophoresis option based on Brock's formulation[10] has been included. Options are available to input thermal gradient, source, pressure, temperature, and leakage rate as functions of time.

PARDISEKO-III[11] uses an iterative procedure in which the initial size distribution is fed into the right-hand side of the integro-differential equation (in the form of a series of size increments) the integration is performed and the time derivative of the new size distribution is used to propagate the distribution to a later time. With this code, there is no constraint to maintain the distribution log-normal, and bimodal distributions are calculated in some cases. However, the use of this code is limited by the fact that it is still being developed.

3.7.3 References

1. L. F. Parsly, Jr. Work Plan: Transient Release from LMFBR Fuel Addendum 1: Investigation of LMFBR Aerosol Behavior in the Aerosol Test Facility ORNL-TM-4875 Addendum 1, January 1976
2. P. Beiriger et. al., SOFIRE-II User Report USAEC Report AI-AEC 13055 Atomics International (1973).
3. P. R. Shire, SPRAY-I - A Combusion Model for Hypothetical Spray Fire Within Containment of a Liquid Metal Fast Breeder Reactor, M. S. Thesis, University of Washington, 1972.
4. M. P. Heisler and K. Mori, SOMIX-I User Manual for the LBL-CDC 7600 Computer, Atomics International (to be published).
5. R. D. Peak, D. D. Stepnewski, "Computational Features of the CACECO Containment Analysis Code," Trans. Am. Nucl. Soc. 21, 274, (1975).
6. B. U. B. Sarma, F. Hayes and R. C. Thompson, Review of Current Sodium Fire Analytical Methods, USERDA Report GEAP-14148 (Sept. 1976).
7. R. S. Hebner, E. V. Vaughan and L. Baurmash, HAA3 User Report, AI-AEC-13038 (1973).
8. L. D. Reed and J. A. Gieseke, HAARM2 Users Manual, BMI-X-665 (1975).
9. W. Stöber et al., "The Aerodynamic Diameter of Latex Aggregates and Asbestos Fibers," Staub-Reinhalt. Luft 30 No. 7, 1–11 (July 1970).
10. J. R. Brock, "On the Theory of Thermal Forces Acting on Aerosol Particles," J. Colloid Sci. 17, 768 (1962).
11. H. Jordan and Chr. Sack, PARDISEKO-III: A Computer Code for Determining the Behavior of Contained Nuclear Aerosols, EURFNR-1268, May 1975.

ORNL/NUREG/TM-124
Dist. Category NRC-7

Internal Distribution

1. R. E. Adams
2. M. Bender
3. H. W. Bertini
4. J. R. Buchanan
6. J. M. Corum
6. W. B. Cottrell
7. F. L. Culler, Jr.
8. J. F. Dearing
9. D. E. Ferguson
10. G. F. Flanagan
11–15. M. H. Fontana
16. P. W. Garrison
17. P. A. Gnadt
18. A. G. Grindell
19. J. T. Han
20. N. Hanus
12. W. O. Harms
22. H. W. Hoffman
23. J. R. Johnston
24. M. A. Karnitz
25. P. R. Kasten
26. M. J. Kelly
27–31. T. S. Kress
32. Milton Levenson
33. R. A. Lorenz
34. R. E. MacPherson
35. F. C. Maienschein
36. A. P. Malinauskas
37. C. A. Mills
38. R. H. Morris
39. F. R. Mynatt
40. F. H. Neill
41. L. C. Oakes
42–43. G. W. Parker
44. L. F. Parsly
45. H. Postma
46. R. J. Ribando
47. J. M. Rochelle
48. E. F. Roy
49. J. P. Sanders
50–51. Myrtleen Sheldon
52. M. J. Skinner
53. A. M. Smith
54. I. Spiewak
55. A. L. Sutton, Jr.
46. D. G. Thomas
47. M. L. Tobias
58. H. E. Trammell
59. D. B. Trauger
60. W. E. Unger
61. J. L. Wantland
62. J. R. Weir
63. J. S. White
64. G. D. Whitman
65. A. L. Wright
66–67. Central Research Library
68. Y-12 Document Reference Section
69–71. Laboratory Records Department
72. Laboratory Records (RC)

External Distribution

73–80. Director, Office of Nuclear Regulatory Research, Nuclear Regulatory Commission, Washington, D.C. 20555
81. Director, Reactor Division, DOE, ORO
82. Director, Research and Technical Support Division, DOE, ORO
83–347. Given distribution as shown in category NRC-7 (25 copies - NTIS)